


For Reference

NOT TO BE TAKEN FROM THIS ROOM

EX LIBRIS
UNIVERSITATIS
ALBERTAENSIS





Digitized by the Internet Archive
in 2022 with funding from
University of Alberta Library

<https://archive.org/details/Green1979>

THE UNIVERSITY OF ALBERTA

A MAGNETIC RESONANCE STUDY OF THE STABILITY AND CONFORMATION
OF THE COMPLEX FORMED BETWEEN THE MANGANESE (II) ION AND
NICOTINAMIDE ADENINE DINUCLEOTIDE PHOSPHATE IN SOLUTION

By



M. KIRK GREEN

A THESIS

SUBMITTED TO THE FACULTY OF GRADUATE STUDIES AND RESEARCH
IN PARTIAL FULFILMENT OF THE REQUIREMENTS FOT THE DEGREE

OF

MASTER OF SCIENCE

DEPARTMENT OF CHEMISTRY

EDMONTON, ALBERTA

SPRING, 1979

TO MARTINA

TO MARTINA

ABSTRACT

Magnetic resonance techniques have been applied to study the stability and conformation of the complex formed between Mn(II) ions and NADP in aqueous solutions at a pH of 7.5 and 20°C. The EPR data indicate that at low Mn(II) ion concentrations, ($[Mn(II)] < 1 \text{ mM}$; $[NADP] = 5 \text{ mM}$), a 1:1 complex is formed with an apparent stability constant $K_1 = 370 \pm 50 \text{ M}^{-1}$ at an ionic strength of 0.22 in the presence of 0.19 M Cl^- . The enthalpy of formation of this complex as measured by EPR techniques is $+ 1.3 \pm 0.2 \text{ Kcal/mol}$. ^{31}P NMR has been used to establish that the complex is characterised by an exchange lifetime of $\tau_M = 4 \times 10^{-6} \text{ sec.}$ and an enthalpy of activation for chemical exchange of $13.7 \pm 0.5 \text{ Kcal/mol}$ under the same conditions. At high Mn(II) ion concentrations, a $Mn(II)_2$ -NADP species, with an apparent stability constant $K_2 = 55 \pm 15 \text{ M}^{-1}$, is present in significant amounts.

The dipolar correlation time (τ_c) for NADP at 20°C was calculated to be $1.7 \times 10^{-10} \text{ sec.}$, based on the measurement of proton longitudinal relaxation time ratios and a literature value of τ_c for NAD. At low Mn(II) ion concentrations, where there is only one distinct binding site for the Mn(II) ion per NADP molecule, the τ_c and relaxation data, together with the measured K_1 value, were used to calculate distances between the Mn(II) ion and the ^{31}P and observable 1H nuclei. These distances are, for

the ^{31}P nuclei: 2'-phosphate, 3.3 Å; low-field linkage phosphate, 3.6 Å; high-field linkage phosphate, 3.7 Å; and for the protons: adenine 8, 3.8 Å; adenine 1', 4.5 Å; adenine 2, 5.0 Å; nicotinamide 2, 5.3 Å; nicotinamide 6, 5.4 Å; nicotinamide 5, 5.5 Å; nicotinamide 1', 5.8 Å; nicotinamide 4, 6.3 Å. Based on these distances, a model is proposed for the Mn(II) complex with NADP. In this complex, the Mn(II) ion is bonded to the oxygen atoms of all three phosphates, and the adenine and nicotinamide bases are 7 to 8 Å apart and parallel. Hence the Mn(II) ion is located between and to one side of the two bases but is distinctly closer to the adenine base. The adenine base is in the anti conformation whereas the nicotinamide moiety can be either in the syn or anti conformation. Hence there is little or no close stacking of the two bases in the complex. The addition of Mg(II) ions to a solution of free NADP caused no observable shift of the aromatic proton peaks of the NMR spectrum, indicating that the rings are similarly oriented in both free and metal-bound NADP.

ACKNOWLEDGEMENTS

I wish to express my gratitude to the following people:

My supervisor, Dr. George Kotowycz, for suggesting the project and his enthusiasm during the course of this research.

Dr. R. E. D. McClung, for his advice on computing and for supplying the weighted non-linear least squares program.

Dr. B. Sykes, for obtaining the ^{31}P T_1 spectra at 110 MHz, and Dr. W. E. Hull for performing the same task at 146 MHz.

Dr. T. Nakashima, Mr. G Bigam, and Mr. T. Brisbane for obtaining spectra and long periods of instruction on using the NMR and EPR instrumentation.

Dr. F. Cantwell, for advice regarding the coenzyme purification.

TABLE OF CONTENTS

CHAPTER		PAGE
ONE	INTRODUCTION	1
TWO	THEORY	7
	(a) EPR	7
	(b) NMR	11
THREE	EXPERIMENTAL	16
	Preparation of Solutions	17
	EPR Experiments	20
	NMR Experiments	22
	(a) Proton T_1 Measurements	22
	(b) ^{31}P T_1 and T_2 Measurements	24
FOUR	RESULTS	25
FIVE	DISCUSSION	39
	BIBLIOGRAPHY	53

LIST OF TABLES

TABLE		PAGE
I	Preparation of solutions for EPR measurements...	18
II	Proton T_1 data and calculated T_{1M} values	35
III	^{31}P T_1 data and calculated T_{1M} values	37
IV	Comparison of T_1 data for NAD and NADP	42
V	T_{1M} values and calculated Mn(II)-proton distances for Mn(II)-NADP	46
VI	T_{1M} values and calculated Mn(II)- ^{31}P nuclei distances for Mn(II)-NADP	47

LIST OF FIGURES

FIGURE		PAGE
1	The structure of NADP	2
2	NADP ^1H NMR spectrum	4
3	^1H inversion recovery spectra for pure NADP..	23
4	EPR spectra of Mn(II) ion solutions with and without NADP	28
5	Scatchard plot of the EPR data, uncorrected for MnCl^+	29
6	Scatchard plot of the EPR data, corrected for MnCl^+	30
7	The temperature dependence of K_1 for Mn(II)- NADP	31
8	The nOe experiment on NADP	32
9	$1/\text{fT}_{1\text{P}}$ <u>vs</u> $1/T$ for the A1' and N1' protons	33
10	$1/\text{fT}_{1\text{P}}$ <u>vs</u> $1/T$ for protons A8, A2, and N2	34
11	$1/\text{fT}_{2\text{P}}$ <u>vs</u> $1/T$ for the ^{31}P nuclei	38

ABBREVIATIONS

A	=	Adenosine
N	=	Nicotinamide
NMN	=	Nicotinamide Mononucleotide
NAD	=	Nicotinamide Adenine Dinucleotide
NADP	=	Nicotinamide Adenine Dinucleotide Phosphate
NADH	=	Reduced NAD
NADPH	=	Reduced NADP
ADP	=	Adenosine Diphosphate
ATP	=	Adenosine Triphosphate
ADPR	=	Adenosine Diphosphoribose
FT	=	Fourier Transform
nOe	=	nuclear Overhauser effect

CHAPTER ONE

INTRODUCTION

The pyridine coenzymes, nicotinamide adenine dinucleotide phosphate (NADP, Figure 1) and nicotinamide adenine dinucleotide (NAD), which differs from NADP only in not having the adenine 2'-ribose phosphate group, are important in the metabolism of all organisms. They are essential coenzymes for the largest group of oxidation-reduction enzymes, the pyridine- dependent dehydrogenases. The reactions of these enzymes involve the oxidation and reduction of the coenzymes: NADP or NAD is reduced and an H^- ion is added to the nicotinamide ring, forming NADPH or NADH respectively, or the reduced form of the coenzyme has a proton removed.

At pH 3, NAD is a neutral molecule and NADP has a charge of -1. The pK for the proton at the A1 nitrogen is 3.9 and there is a pK of 6.0 for the deprotonation of the 2'-phosphate of NADP (Sarma and Mynott, 1972). Thus, at neutral pH, the ionization of the phosphate groups of these molecules is essentially complete and the binding of metal ions to the coenzymes is a possibility.

Divalent metal cations, especially Zn(II), are required for many pyridine-linked enzymes (Lehninger, 1975), and although an enzyme requiring a complex of a metal cation and an oxidized pyridine nucleotide is not known, in at

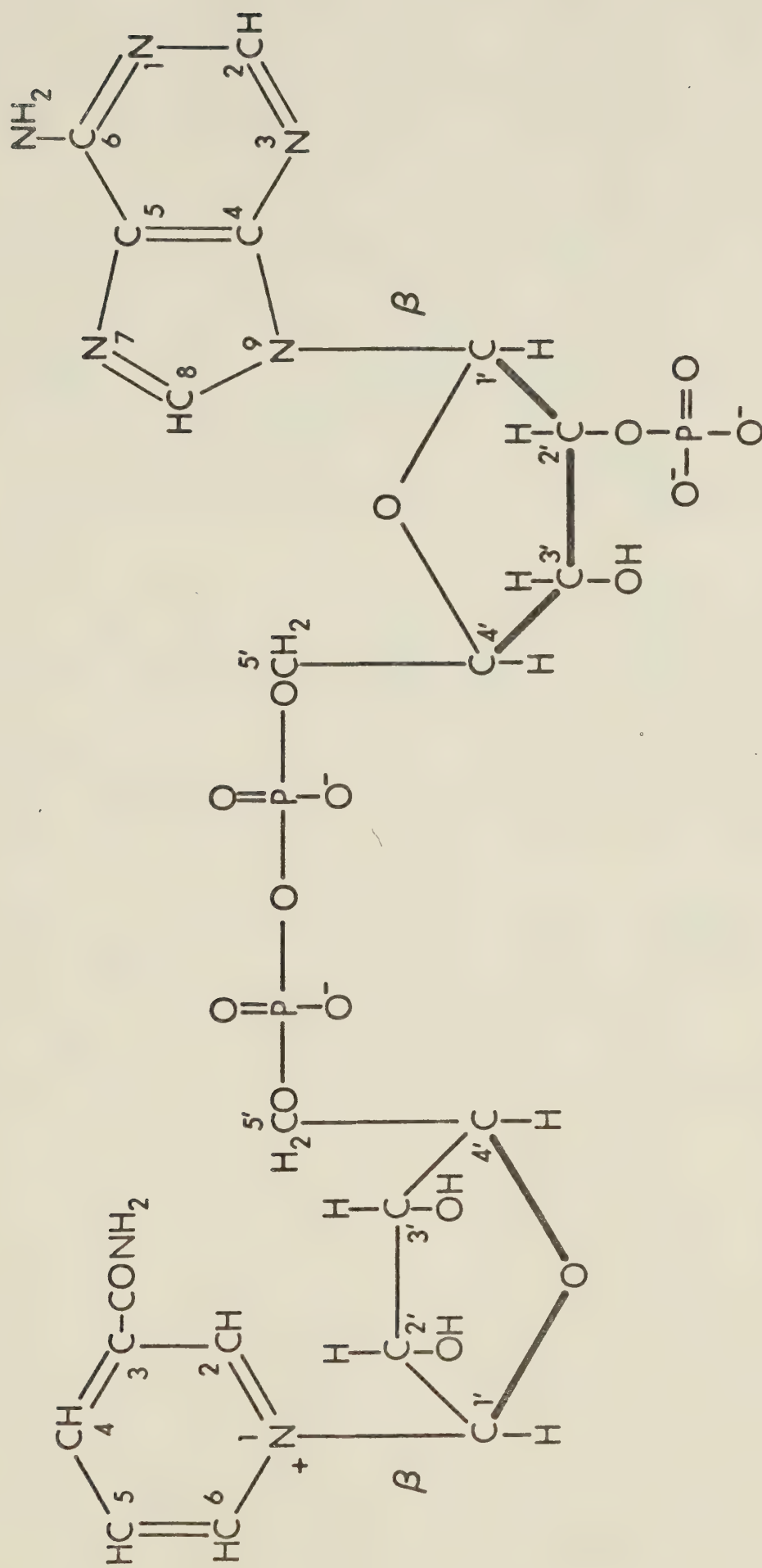


FIGURE 1. The structure of NADP at pH 7.5.

least one case the Mn(II)- NADPH complex is required for an enzymatic reaction (Maloney and Dennis, 1977).

The conformation of a substrate or substrate-metal ion complex in solution is generally unrelated to the conformation of the substrate when bound to the enzyme (Mildvan and Gupta, 1978). However, the solution conformation of the substrate or complex may be of interest in assessing conformational changes that take place on binding to an enzyme or the affinity of the enzyme for the substrate.

The solution conformations of NADP and NAD have extensively studied by nuclear magnetic resonance (NMR) techniques (Jardetzky and Wade-Jardetzky, 1966; McDonald et al., 1972; Blumenstein and Raftery, 1973; Egan et al., 1975; Bose and Sarma, 1975; Zens et al., 1976; and references therein). A spectrum of NADP is shown in Figure 2. Chemical shift measurements imply that these coenzymes exist in an equilibrium of folded and extended forms at room temperature and neutral pH (Jardetzky and Wade-Jardetzky, 1966; McDonald et al., 1972). However, the nature of the unfolded form is unclear. Czeisler and Hollis (1975) found that N-methyl nicotinamide and adenosine diphosphate (ADP) associate in solution, and concluded that the adenine and nicotinamide rings must associate in folded NAD. Sarma and Mynott (1975) proposed a model in which the two rings are stacked and are 3.5 \AA apart, but Ellis and coworkers (Zens et al., 1976) concluded from their studies that the rings

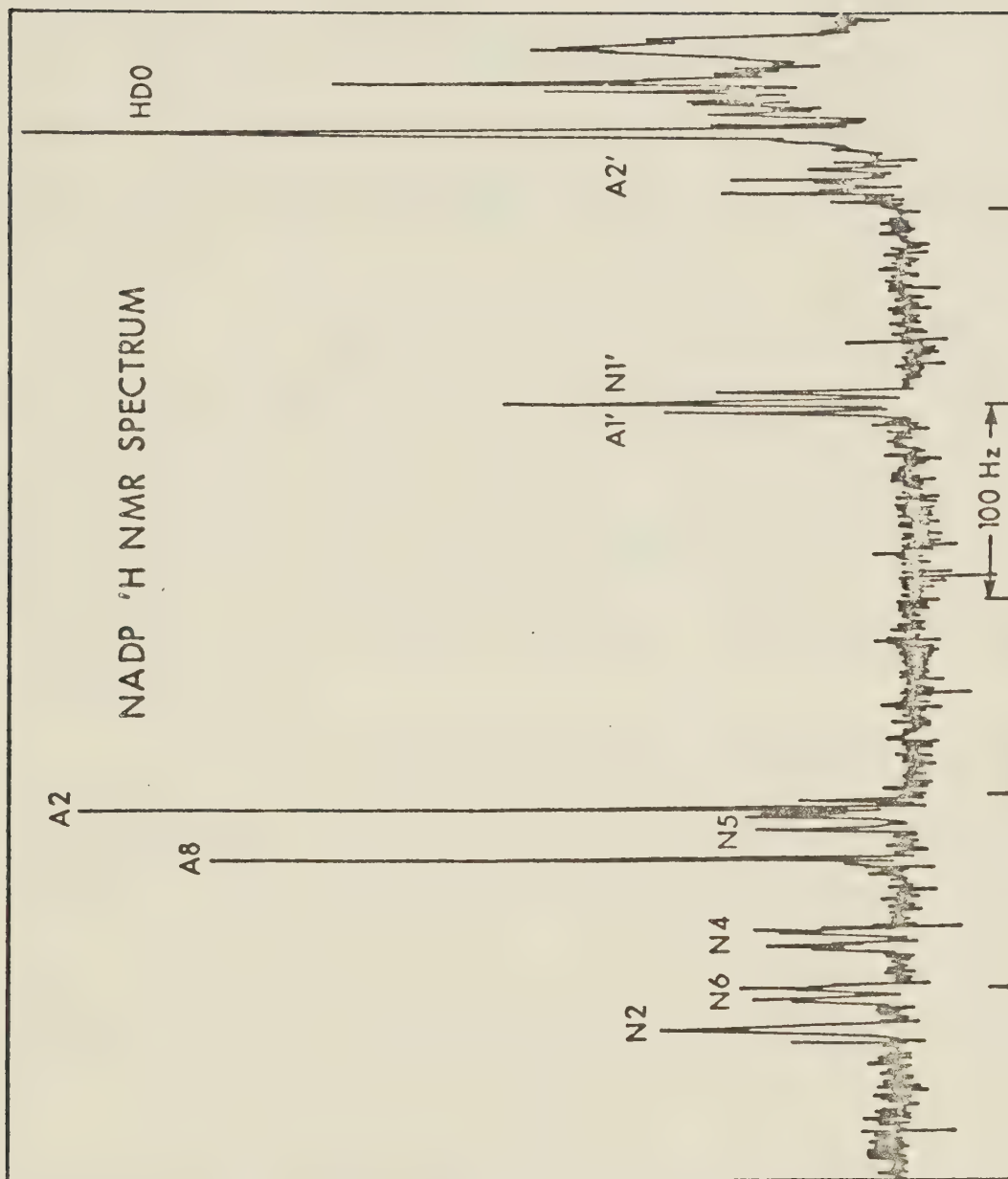


FIGURE 2. The FT NMR spectrum of NADP (5 mM). The HDO peak is at $\delta = 4.8$.
100 pulses were used to obtain this spectrum.

do not approach each other closer than 4.5 \AA for a time comparable to the rotational correlation time of NAD.

X-ray studies (Saenger et al., 1977) show that in the solid state, Li(I)-NAD is extended with adenine stacked intermolecularly on nicotinamide and the Li(I) ion is coordinated to the A7 nitrogen and to three of the phosphate oxygens. NMR studies of Co(II) binding to NADP (Torreilles and Crastes de Paulet, 1973; Torreilles et al., 1975) show direct binding of Co(II) to the phosphate linkage in solution.

The stability constant for the Mn(II)-NADP complex has been determined to be approximately 800 M^{-1} (Maloney and Dennis, 1977; Coleman, 1972) near neutral pH and at ionic strength less than or equal to 0.1. It is strongly dependent on pH near pH 6.0 where the 2'-phosphate group ionizes.

In the present study, the Mn(II) ion complexes with NADP have been studied using electron paramagnetic resonance (EPR) and ^1H and ^{31}P NMR relaxation techniques in an effort to elucidate the structure of these complexes and the solution conformation of free NADP. The apparent stability constant and number of binding sites have been determined from EPR data, based on the method of Cohn and Townsend (1954). This information, together with the ^1H and ^{31}P relaxation data, has been used to calculate the distances from the bound Mn(II) ion to eight of the NADP protons and the three ^{31}P nuclei in the aid of a correla-

tion time derived from a literature value for NAD. These distances give a picture of the Mn(II)-NADP complex in solution.

CHAPTER TWO

THEORY

(a) EPR

Although the binding constant for the Mn(II)-NADP complex has been determined by other workers (Coleman, 1972; Maloney and Dennis, 1977), the binding constant is, of course, dependent on experimental conditions, and as the conditions of this study were somewhat different than those in the literature, it was necessary to measure the binding constant and number of binding sites under the conditions of the present study.

The binding of Mn(II) to a small molecule may be conveniently monitored by measuring the intensity of the EPR spectrum of the Mn(II) ion in the presence and absence of the molecule of interest since the intensity of the manganese signal drops drastically on binding, and the signal observed is essentially only due to the free Mn(II) (Cohn and Townsend, 1954). This loss of intensity is due to a decrease in the transverse electronic relaxation time (T_{2e}) of the Mn(II) ion which occurs on binding (Reed et al., 1971).

In the case of a metal ion binding to n equivalent sites on a molecule, data on the concentration dependence of binding is readily analysed to yield the number of binding sites and the stability constant, K_s , defined as:

$$K_s = \frac{ML}{L_f^n M_f} \quad (1)$$

where ML = concentration of filled binding sites

M_f = concentration of the free metal ion

L_f = concentration of the free ligand

Since $ML = M_b$, the concentration of metal ion bound,
and $nL_f = nL_t - M_b$, where L_t = total ligand concentration,
equation (1) may be written as:

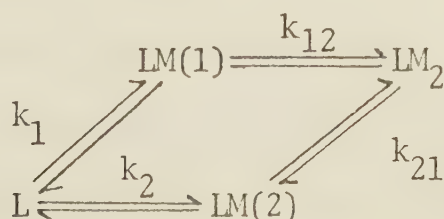
$$K_s = \frac{M_b}{(nL_t - M_b)M_f} = \frac{M_b}{L_t(n - M_b/L_t)M_f} = \frac{\bar{\mu}}{(n - \bar{\mu})M_f} \quad (2)$$

where $\bar{\mu} = M_b/L_t$ is the average number of metal ions bound per ligand. Equation (2) may be written as:

$$\bar{\mu}/M_f = K_s(n - \bar{\mu}) \quad (3)$$

Hence a plot of $\bar{\mu}/M_f$ versus $\bar{\mu}$ yields a straight line with a y intercept = $K_s n$ and an x intercept of n , with a slope of $-K_s$. This is known as a Scatchard plot.

A plot of the present EPR data, however, gave a curved line with an x intercept of about 2, indicating two non-equivalent sites. The binding scheme for the case of two non-equivalent sites may be represented as shown:



where L = the free ligand molecule

$LM(1)$ = the ligand with a metal bound at site (1)

LM(2) = the ligand with a metal bound at site (2)

LM₂ = the ligand metal bound at both sites and k_1 , k_2 ,

k_{12} , and k_{21} are the microscopic binding constants.

If the two binding sites do not interact, that is, binding at one site does not affect the other, then $k_1 = k_{21}$ and $k_2 = k_{12}$ and the microscopic binding constants may be extracted from a fit to the following equation (Villafranca and Mildvan, 1971):

$$\frac{\bar{\mu}}{\bar{M}_f} = k_1 + k_2 + 2k_1k_2M_f - (k_1 + k_2 + k_1k_2M_f)\bar{\mu} \quad (4)$$

If the sites do interact, and microscopic binding constants are difficult to measure, then the macroscopic binding constants may still be obtained. Deranleau (1969) gives the equation relating the UV absorption to the macroscopic binding constants K_1 and K_2 for the general case (sites may or may not interact):

$$\frac{A}{2\epsilon L_t} = \frac{1}{2} \times \frac{K_1M_f + 2K_1K_2M_f^2}{1 + K_1M_f + K_1K_2M_f^2} = s \quad (5)$$

where A = absorbance

s = saturation fraction - the fraction of total sites occupied

ϵ = extinction coefficient of LM₂

K_1 = first macroscopic binding constant = $k_1 + k_2$

K_2 = second macroscopic binding constant and

$$1/K_2 = 1/k_1 + 1/k_{12} = 1/k_2 + 1/k_{21}$$

Here it has been assumed that only the complexes absorb

and that the two LM species have equal extinction coefficients equal to $\epsilon/2$.

For the EPR case, this equation may be applied for the case where the bound Mn(II) ion does not contribute to the EPR signal intensity. This is a good approximation for metal-nucleotide complexes (Cohn and Townsend, 1954). For two binding sites, $\bar{\mu} = 2s$, and equation (5) may be rearranged as follows:

$$\frac{\bar{\mu}}{M_f} = \frac{K_1 + 2K_1K_2M_f}{1 + K_1M_f + K_1K_2M_f^2} \quad (6)$$

Once K_1 and K_2 are determined, an independent determination of one of the microscopic binding constants will allow the calculation of all the microscopic constants of the system.

Note that for two interacting sites, the x and y intercepts of a Scatchard plot ($\bar{\mu}/M_f$ vs $\bar{\mu}$) have meanings analogous to those for the Scatchard plot in the case of n equivalent and independent binding sites: the y intercept (that is, the value of $\bar{\mu}/M_f$ as $M_f \rightarrow 0$) equals K_1 , and the x intercept (the value of $\bar{\mu}$ as $M_f \rightarrow \infty$) equals 2, the number of binding sites.

(b) NMR

The equations for the relaxation times of a nucleus bound near a paramagnetic species have been derived by Solomon (1955) and Bloembergen (Solomon and Bloembergen, 1956) and modified by Connick and Fiat (1966) and Reuben et al. (1970). These equations are written as follows, assuming $\omega_S \gg \omega_I$:

$$T_{1M}^{-1} = \frac{2}{15} \frac{S(S+1) g^2 \beta^2 \gamma_I^2}{r^6} \left(\frac{3\tau_{c1}}{1 + \omega_I^2 \tau_{c1}^2} + \frac{7\tau_{c2}}{1 + \omega_S^2 \tau_{c2}^2} \right) + \frac{2}{3} S(S+1) \left(\frac{A^2}{h^2} \right) \left(\frac{\tau_{e2}}{1 + \omega_S^2 \tau_{e2}^2} \right) \quad (7)$$

$$T_{2M}^{-1} = \frac{1}{15} \frac{S(S+1) g^2 \beta^2 \gamma_I^2}{r^6} \left(4\tau_{c1} + \frac{3\tau_{c1}}{1 + \omega_I^2 \tau_{c1}^2} + \frac{13\tau_{c2}}{1 + \omega_S^2 \tau_{c2}^2} \right) + \frac{1}{3} S(S+1) \left(\frac{A^2}{h^2} \right) \left(\tau_{e1} + \frac{\tau_{e2}}{1 + \omega_S^2 \tau_{e2}^2} \right) \quad (8)$$

where S = spin of the paramagnetic species

ω_I = magnetogyric ratio of nucleus I

g = electron g factor

β = Bohr magneton

r = distance from nucleus to the paramagnetic ion

ω_S = angular electron precession frequency

γ_I = angular nuclear precession frequency

$\frac{A}{\hbar}$ = scalar coupling constant between the nucleus and
the paramagnetic species

τ_{ci} = the dipolar correlation time

= $1/\tau_R + 1/\tau_{ei} = 1/\tau_R + 1/\tau_M + 1/T_{ie}$ and

τ_R = rotational correlation time

τ_M = exchange lifetime; mean time that a ligand is bound

T_{ie} = electron relaxation time

Strictly speaking, the equation should be modified to take into account the fact that the transverse and longitudinal electron relaxation times for Mn(II) are each characterized by three relaxation times (Rubenstein et al., 1971).

Fortunately, the magnitudes of A/\hbar and τ_e for octahedral Mn(II) complexes are such that (Rubenstein et al., 1971; Swift, 1973; Dwek, 1975) the second (scalar) term in equation (7) is negligible and furthermore, for a small molecule such as NADP, the magnitudes of the electron relaxation times and the exchange lifetime for Mn(II) are generally much larger than τ_R . Thus, to a good approximation $1/\tau_c = 1/\tau_R$ and there is only one correlation time to consider. In addition, at 100 MHz, for a molecule as small as NADP, $\omega_S \tau_c \gg 1$, so that equation (7) may be written as:

$$\frac{1}{T_{1M}} = \frac{2}{15} \frac{\gamma_I^2 g^2 S(S+1) \beta^2}{r^6} \left(\frac{3\tau_R}{1 + \omega_I^2 \tau_R^2} \right) \quad (9)$$

For nuclei relaxed by Mn(II), equation (9) may be written as:

$$\frac{1}{T_{1M}} = \left(\frac{C}{r} \right)^6 \frac{\tau_R}{1 + \omega_I^2 \tau_R^2} \quad (10)$$

where C is a constant equal to 812 for protons and 601 for ^{31}P nuclei. For a system in which not all of the ligand molecules are bound to the paramagnetic species, T_{iM} ($i = 1$ or 2) is related to the observed relaxation time, $T_{i,Mn}$ by (Luz and Meiboom, 1964; Swift and Connick, 1962):

$$\frac{1}{T_{1,Mn}} - \frac{1}{T_{1,0}} = \frac{1}{T_{1P}} = \frac{f}{T_{1M} + \tau_M} + \frac{1}{T_{1,o.s.}} \quad (11)$$

$$\begin{aligned} \frac{1}{T_{2,Mn}} - \frac{1}{T_{2,0}} = \frac{1}{T_{2P}} = \frac{1}{\tau_M} & \left[\frac{\frac{1}{T_{2M}} \frac{1}{T_{2M}} + \frac{1}{\tau_M} + \Delta\omega_M^2}{\frac{1}{T_{2M}} + \frac{1}{\tau_M} + \Delta\omega_M^2} \right] \\ & + \frac{1}{T_{2,o.s.}} \end{aligned} \quad (12)$$

where $1/T_{iP}$ = contribution of the paramagnetic species to the relaxation rate

$1/T_{i,o.s.}$ = contribution to the relaxation rate by the paramagnetic species not directly bound (outer sphere relaxation)

f = fraction of nuclei bound to paramagnetic species

$\Delta\omega_M$ = chemical shift difference between bound and free nuclei

In Mn(II) systems, $\frac{1}{T_{2M}}^2 \gg \Delta\omega_M^2$ and hence equation (12)

reduces to :

$$\frac{1}{T_{2P}} = \frac{1}{T_{2M} + \tau_M} + \frac{1}{T_{2,o.s.}} \quad (13)$$

It can be seen from equation (9) and (11) that distances may be obtained from T_{1P} measurements only if $T_{1M} \gg \tau_M$. If $\tau_M \ll T_{1M}$ (fast exchange region) and $1/T_{i,o.s.} \ll 1/fT_{iP}$, then $1/fT_{iP} \propto \tau_R$ for $\omega_I \tau_R \ll 1$. Since the temperature dependence of τ_R is given by the following equation (Dwek, 1975):

$$\tau_R = \tau_R^o \exp \frac{E_R}{RT} \quad (14)$$

where τ_R^o = a constant

E_R = activation energy associated with the rotational motion

R = the ideal gas constant

T = temperature ($^{\circ}K$)

a plot of $\ln 1/fT_{iP}$ versus $1/T$ will give a straight line of positive slope E_R/R . On the other hand, if $\tau_M \gg T_{1M}$ (slow exchange conditions) and $1/T_{i,o.s.} \ll 1/fT_{iP}$, then $1/fT_{iP} \propto 1/\tau_M$. The temperature dependence of τ_M is given by (Dwek, 1975):

$$\frac{1}{\tau_M} = \frac{kT}{h} \exp \left[\frac{-\Delta H^{\ddagger}}{RT} + \frac{\Delta S^{\ddagger}}{R} \right] \quad (15)$$

where h = Planck's constant

k = Boltzmann's constant

ΔH^\ddagger = enthalpy of activation for chemical exchange

ΔS^\ddagger = entropy of activation for chemical exchange

In this case, a plot of $\ln(1/fT_{iP})$ versus $1/T$ will give a line of negative slope and a plot of $\ln(1/fT_{iP} - kT/h)$ versus $1/T$ will give a straight line of slope $-\Delta H^\ddagger/R$.

CHAPTER THREE

EXPERIMENTAL

NAD (free acid) and NADP (monosodium salt) from Sigma Chemical Co. and N-ethyl morpholine from Eastman Organic Chemical Co. were purified as described below. $\text{MnCl}_2 \cdot 4\text{H}_2\text{O}$ from Fisher Scientific Co., and KCl, from J.T. Baker Co., were used without further purification.

The NAD and NADP were purified by passing a solution of the coenzyme through a 1 x 20 cm column of Chelex 100 (from Bio-Rad Laboratories) which had been rinsed with HCl, methanol, and NaOH followed by equilibration with NaH_2PO_4 buffer at pH 7 and extensive rinsing with doubly deionized distilled water until the eluted water was at pH >9. After purification, the coenzyme was lyophilized, then lyophilized 2-3 times more from D_2O and stored frozen in a desiccator. The ^{31}P linewidths of undegassed samples which were purified in this manner were ≤ 1.5 Hz.

The D_2O was 99.7% substituted, and was vacuum distilled. The N-ethyl morpholine was used without purification for the EPR experiments, and was vacuum distilled for the NMR experiments.

All glassware was cleaned thoroughly to eliminate paramagnetic contamination of the samples: items were washed, soaked in 20% nitric acid for at least 8 hours, rinsed three times with distilled water, rinsed with EDTA solution, rinsed three more times with distilled water, and then rinsed three times with doubly distilled water.

PREPARATION OF SOLUTIONS

Stock solutions of $\text{MnCl}_2 \cdot 4\text{H}_2\text{O}$ in 0.100 M KCl in H_2O were made up with the Mn(II) concentration varying from 2×10^{-3} M to 4×10^{-2} M and were used for all experiments. The small amount of H_2O introduced into the NMR samples by using these stock solutions did not affect the present experiments. Stock solutions of 0.250 M N-ethyl morpholine in 0.100 M KCl (pH was adjusted to 7.52 by addition of HCl and NaOH), and 0.365 M KCl were prepared in H_2O for the EPR experiments and in D_2O for the NMR measurements. NADP and NAD stock solutions at a concentration of about 0.25 M in 0.100 M KCl were prepared for 2 or 3 samples at a time. For each coenzyme stock solution, the concentration was measured by UV absorption ($\epsilon = 1.80 \times 10^4$ at 260 nm and pH 7.4; Pabst, 1954) and the stock solution was stored frozen.

After several preliminary experiments, the following procedure was devised for preparing the EPR samples: All samples were made up with a nominal ionic strength of 0.233 ± 0.005 and a Cl^- ion concentration of 0.203 ± 0.005 M (see Table I). For each experimental point, a standard solution was prepared using 1.00 ml of N-ethyl morpholine stock solution, 0.250-2.50 ml of MnCl_2 stock solution, and zero to 1.25 ml of 0.365 M KCl in a 5 ml volumetric flask which was then filled to volume with 0.100 M KCl. For the sample solution, identical amounts of the stock solutions were measured into a 5 ml beaker, the pH measured on an Orion 801 digital pH meter, 0.250 to 1.00 ml of coenzyme stock solution added, and the pH (which changed by less than 0.15 pH units on the addition) was readjusted with dilute NaOH (less than 50 μl was required). The beaker was then

TABLE I. Preparation of solutions for the EPR experiments

Sample	Vol. of Mn(II) stock (ml)	Vol. of NADP stock (ml)	Vol. of 0.365 M KCl (ml)	Ionic strength due to reagent				Cl ⁻ Conc.
				Mn(II)Cl ₂	NADP	N-ethyl morpho- line Cl	KCl Total	
1	2.50 #1	.250	0	.090	.0071	.039	.100 .236	.199
2	2.50 #1	.250	0	.090	.0071	.039	.100 .236	.199
3	2.00 #2	.500	.500	.048	.0141	"	.127 .228	.198
4	1.50 #2	.500	.750	.036	.0141	"	.140 .229	.203
5	1.00 #2	.500	1.00	.024	.0141	"	.153 .230	.208
6	.750 #2	1.00	1.00	.018	.0229	"	.153 .233	.204
7	.500 #2	1.00	1.00	.012	.0282	"	.153 .232	.200
8	1.00 #3	1.00	1.00	.0096	.0275	"	.153 .229	.198
9	.500 #3	1.00	1.25	.0048	.0282	"	.166 .238	.208
10	.500 #4	1.00	1.25	.0024	.0282	"	.166 .236	.207

(a) Concentrations of the Mn(II) stock solutions are: #1 = 0.0600 M; #2 = 0.0400 M; #3 = 0.0160 M; #4 = 0.00800 M.

emptied into another 5 ml volumetric flask. The beaker and pH probe were then rinsed into this flask, and the flask filled to volume with 0.100 M KCl. All samples and standard solutions had a measured pH of 7.52 ± 0.10 . The Mn(II) ion concentrations varied from 0.8 mM to 20 mM and the NADP concentrations varied between 1.33 mM and 4.5 mM.

After mixing, the sample and standard solutions were then each drawn up into a 25 μ l or 50 μ l disposable micropipet and the micropipet sealed with wax at both ends. The micropipet was then placed in the EPR spectrometer and a spectrum recorded. Samples with high Mn(II) concentration (6 mM or greater) started to precipitate after 2 to 3 days, and so were run immediately after mixing. EPR signal intensity ratios (sample to standard) remained constant for at least several hours after mixing.

For the NMR experiments, the ionic strength (0.219) and the Cl^- ion concentration (0.193 M) were slightly different from those for the EPR experiments, but not enough to significantly affect the results. A Mn(II) ion stock solution was prepared by diluting a portion of the 2.00 M Mn(II) stock used for the EPR in D_2O . Unlike the EPR samples, NaOH was not added after the addition of the NADP; the measured pH was about 7.6 (pD 8.0, Lumry et al., 1951) and it was felt this was high enough that the risk of contamination involved by addition of another reagent was not worthwhile. The NADP concentration was about 4.5 mM for all samples, and the Mn(II) concentration varied from 0 to 6.0 mM. The concentration of NADP in all samples was measured by UV absorption.

The temperature dependence of binding was studied by EPR

at the lowest concentration of Mn(II) used for the Scatchard plot experiment (0.800 mM). A low concentration was used so that only binding due to the first macroscopic binding constant would be observed. The temperature dependence of $1/T_{1P}$ for protons was studied using a solution with an optimum concentration of Mn(II) for measuring the relaxation of the fastest-relaxing nucleus (1.0 μ M). The concentration of Mn(II) chosen for the ^{31}P linewidth temperature study balanced two requirements: low concentration for readily observable signals, and high concentration for a large amount of broadening. The nuclear Overhauser effect (NOE) experiment was run at 304°K on a sample similar to the other NMR samples, except that the NADP concentration was 0.05 M and the sample was vacuum degassed.

EPR EXPERIMENTS

EPR measurements were obtained using a Bruker B-ER 400X EPR console (X band) interfaced with a Varian V3601 12 inch magnet and a Varian VFR Fieldial Controller. Points for the Scatchard plot were measured with room temperature N_2 (293 °K) blown through the cavity. Most of the spectra were obtained using a Varian double resonance cavity with the intensity ratios of the sample and standard being taken as the average ratio of all six Mn(II) ion peak heights for both possible arrangements of the samples (sample in front with standard in back or vice-versa). Some of the spectra taken for the plot and those for the temperature dependence study were run using a Bruker single cavity which gave much greater sensitivity and equal reproducibility. For the temperature study, the temperature

was controlled using a Bruker B-ER 100/700 temperature control unit.

$\bar{\mu}$ and $\bar{\mu}/Mn_f$ ($Mn_f = [Mn(II)]_{free}$) were calculated from the intensity ratio using the following expression:

$$Mn_f = \frac{\text{signal of free Mn(II)}}{\text{signal of total Mn(II)}} \times Mn_t = \frac{\text{signal of sample}}{\text{signal of blank}} \times Mn_t \quad (16)$$

where $Mn_t = [Mn(II)]_{total}$

Hence it is possible to calculate the concentration of Mn(II) bound to NADP, Mn_b , from a measurement of the relative signal intensities and thus $\bar{\mu}$ and $\bar{\mu}/Mn_f$ if $[Mn(II)]_{total}$ is known.

Because Mn(II) ions are known to bind Cl^- ions with a K_s for $MnCl^+$ of $3.7 M^{-1}$ (Gryzbowski et al., 1970), points were also calculated corrected for Cl^- binding. This was done according to the following procedure. Using the known value of K_s and total concentrations of Mn(II) and Cl^- , the actual free Mn(II) concentration in the standard solution was calculated, and assuming that $MnCl^+$ does not contribute to the EPR signal intensity, the free Mn(II) concentration in the sample was calculated from signal intensities. (In a separate experiment, the EPR spectrum of the Mn(II) ion in saturated KCl was obtained and the results indicate that the $MnCl^+$ ion gives rise to some signal intensity, but it is relatively small.) This value for the free Mn(II) ion concentration was then used to calculate the concentration of $MnCl^+$ and then the actual amount of Mn(II) bound to NADP. The possibility of Mn(II) ion binding to N-ethyl morpholine was ignored as the K_s for this interaction is known to be small (O'Sullivan and Cohn, 1966).

NMR EXPERIMENTS

(a) Proton T_1 measurements

Proton magnetic resonance spectra at 100 MHz using the deuterium resonance of D_2O as the lock signal were obtained using a Varian HA-100-15 NMR spectrometer interfaced with the Digilab FTS/NMR-3 Fourier transform system, the pulse unit (FTS/NMR 400-2) and the Nova 1200 computer. The temperature was maintained using a Bruker B-ST 100/700 temperature control unit. T_1 measurements were carried out using the 180° - τ - 90° inversion-recovery pulse sequence (50-100 pulses). A typical set of spectra so obtained is shown in Figure 3. For most experiments, the residual HDO peak was saturated using a Hewlett-Packard HP 5100B frequency synthesizer, which improved the signal-to-noise ratio with no apparent change in the measured T_1 values. Peak height measurements from the spectra were used for the T_1 calculation; for the nicotinamide N4 and N6 proton resonances, average peak heights of the doublets were used, but for the nicotinamide N5 and N1' and the adenine A1' proton resonances, only one peak could be used due to the overlap of signals. Data for the amplitude and τ were computer simulated to the equation governing T_1 relaxation, $A = A_0(1-2\exp(-\tau/T_1))$ to obtain a value for T_1 with an uncertainty of $\pm 10\%$.

(b) ^{31}P T_1 and T_2 measurements

^{31}P linewidths of NADP in the presence and absence of Mn(II) (0.33 μM) were measured on Bruker HFX-90 NMR spectrometer at four temperatures. Temperature was controlled using the Bruker B-ST 100/700 unit. $1/fT_2$ for each resonance was calculated from the linewidths:

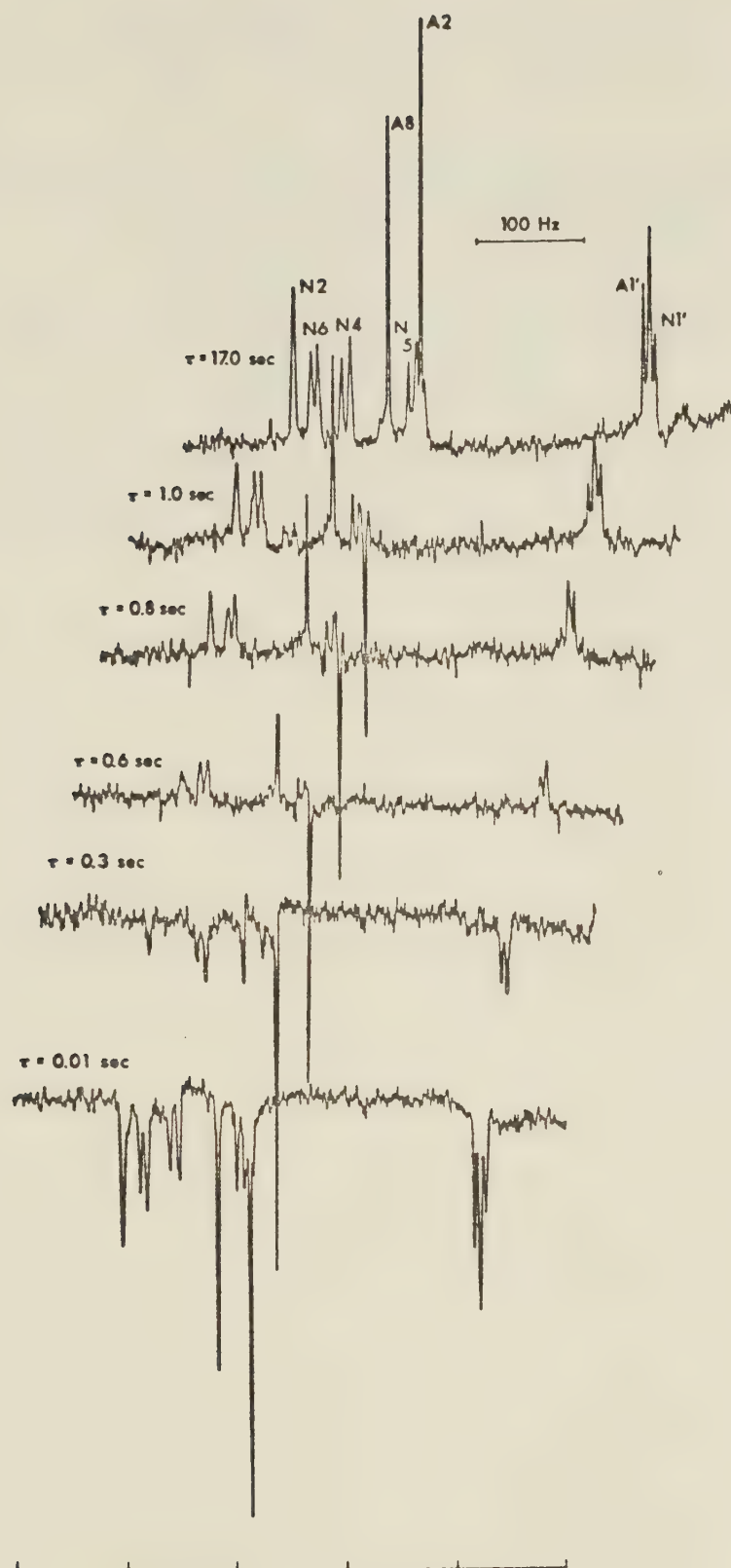


FIGURE 3. ^1H inversion recovery spectra for pure NADP.
Each spectrum represents 50 pulses.

$$\frac{1}{T_{2P}} = \frac{\pi}{T} (\Delta\nu_{1/2, \text{Mn}} - \Delta\nu_{1/2, 0})$$

where $\Delta\nu_{1/2, \text{Mn}}$ = linewidth at half-height of the resonance in
the solution containing Mn(II) ions

$\Delta\nu_{1/2, 0}$ = linewidth at half-height of the resonance in
the pure NADP solution

^{31}P T_1 measurements were run at a frequency of 110 MHz
(28°C) and at a frequency of 146 MHz (25°C).

CHAPTER FOUR

RESULTS

Typical EPR spectra of Mn(II) ions with and without NADP added to the solution are shown in Figure 4. The intensity of the signal decreases in the presence of NADP due to binding. It proved impossible to detect a signal due to the Mn(II)-NADP complex; at high ratio of Mn(II) to NADP concentration, the free Mn(II) signal was very strong (due to the weak binding constant) and at low concentration ratios, the high concentration of NADP resulted in extensive stacking and increased the solution viscosity; stacking and increased viscosity would both be expected to broaden the signal, making it difficult to observe.

Figures 5 and 6 are Scatchard plots based on the EPR data, uncorrected and corrected for the presence of MnCl^+ , respectively. The solid lines represent the best computer fits obtained assuming 2 interacting binding sites. A weighted non-linear least squares program was used, with the points weighted by $1/\sigma^2$, where σ is the effective error assuming a 2% error in the ratio M_f/M_t . The temperature dependence of the first macroscopic binding constant is shown in Figure 7.

If two nuclei are close to each other, the intensity of the NMR signal of one may change if the other is irradiated at its resonant frequency. This effect is termed the nuclear Overhauser effect (nOe). In the nOe experiment performed in this work, (figure 8) irradiation at the N2 proton peak position caused an increase in intensity of the right-hand (upfield) peak of the anomeric triplet (actually, two doublets, corresponding to A1' and N1', are super-

imposed), indicating that for NADP under the conditions of this study, the N1' doublet is to high field of the A1' doublet. All of the other proton resonances labelled have been assigned previously (Jardetzky and Wade-Jardetzky, 1966; Sarma and Mynott, 1973).

The temperature dependence of $1/fT_{1P}$ for five of the protons is shown in Figures 9 and 10. Plots for the three other observable protons are not shown because of the large error involved resulting from using a metal concentration which was not high enough for accurate measurement of $1/fT_{1P}$ for these protons.

The proton decoupled ^{31}P spectrum of NADP obtained in this work is essentially the same as that reported previously (Blumenstein and Raftery, 1972; Sarma and Mynott, 1972): one peak at low field corresponding to the ^{31}P of the 2'-phosphate group, near the inorganic phosphate region, and an AB quartet about 13 ppm to high field of this resonance, corresponding to the two ^{31}P nuclei of the phosphate linkage. An undecoupled spectrum was obtained at 110 MHz, and the ^{31}P -H coupling constants between the linkage ^{31}P nuclei and the non-equivalent C5' protons were measured to be 4.6 Hz and 3.2 Hz for the low field ^{31}P resonance of the quartet, and 7.4 Hz and 4.4 Hz for the high field resonance. Unfortunately, these values do not correspond closely to the coupling constants obtained from the proton spectrum by Bose and Sarma (1975) and an unambiguous assignment of the ^{31}P resonances to the respective linkage ^{31}P nuclei cannot be made at this time.

The T_1 values obtained for the various Mn(II)-NADP solutions together with the calculated T_{1M} values are listed in Table II for the protons and Table III for the ^{31}P nuclei.

Finally, the temperature dependence of $1/fT_{2P}$ for the ^{31}P nuclei is shown in Figure 11. One line was drawn to fit the points for both of the linkage phosphate ^{31}P nuclei, because linewidths for these nuclei could not be separately resolved in the spectra of the Mn(II)-containing sample. A separate plot (not shown) of $\ln(1/fT_{1P} - kT/h)$ versus $1/T$ gave ΔH^\ddagger for all 3 nuclei to be 13.7 ± 0.5 Kcal/mol.

Comparison of the T_1 values for the N-ethyl morpholine proton resonances in a pure NADP solution with those measured for N-ethyl morpholine in a solution containing $1.0 \mu\text{M}$ Mn(II) ions gave a value of $1/T_{1P}$ for these resonances of about 0.05 sec^{-1} . As N-ethyl morpholine complexes very weakly with Mn(II) ions, (O'Sullivan and Cohn, 1966) this value may be regarded as an upper limit on $1/T_{1,o.s.}$ for the NADP protons. A comparison of this number with $1/T_{1P}$ for the NADP protons under the same conditions shows that outer sphere relaxation will not significantly affect any of the distances calculated from $1/T_{1P}$.

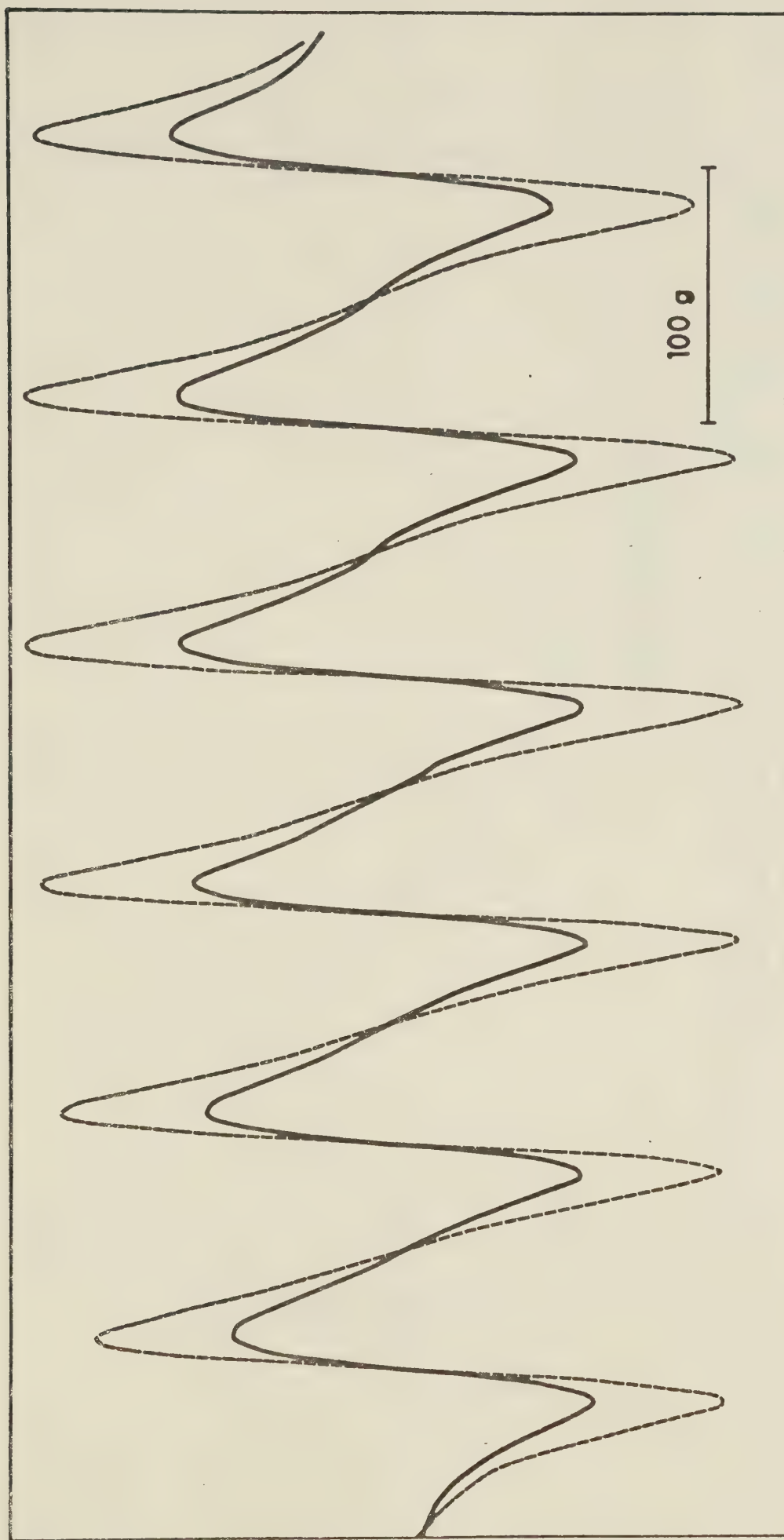


FIGURE 4. EPR spectra of Mn(II) ion solutions with (—) and without (----) NADP added. The experimental conditions are: $[\text{Mn(II)}]_{\text{total}} = 6.0 \text{ mM}$; $[\text{NADP}] = 3.82 \text{ mM}$.

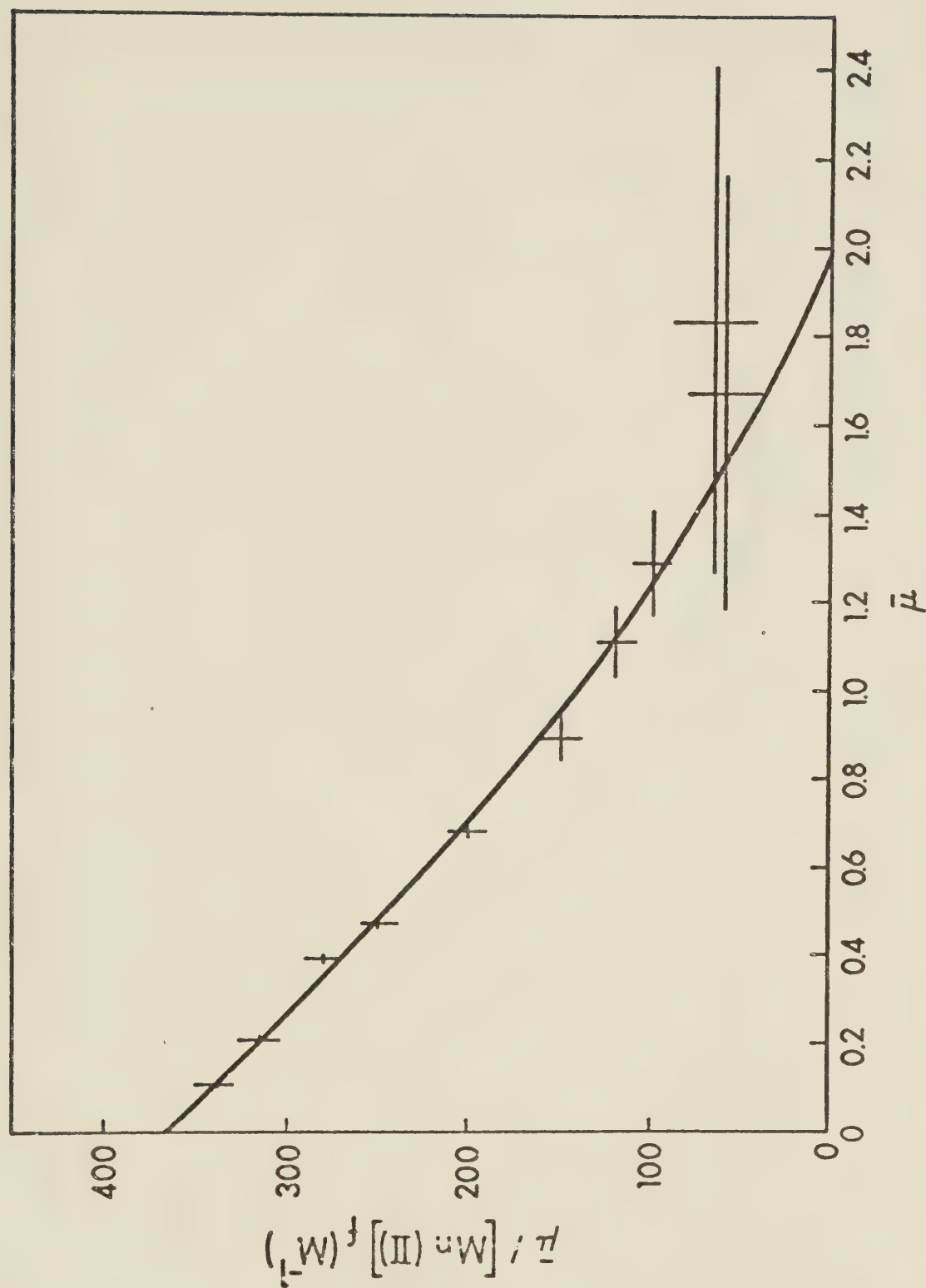


FIGURE 5. The Scatchard plot of the EPR data, uncorrected for $MnCl^+$. The error limits are calculated assuming an error of $\pm 2\%$ in determining the ratio $[Mn(II)]_{free}/[Mn(II)]_{total}$. The solid line represents the best fit assuming two interacting binding sites.

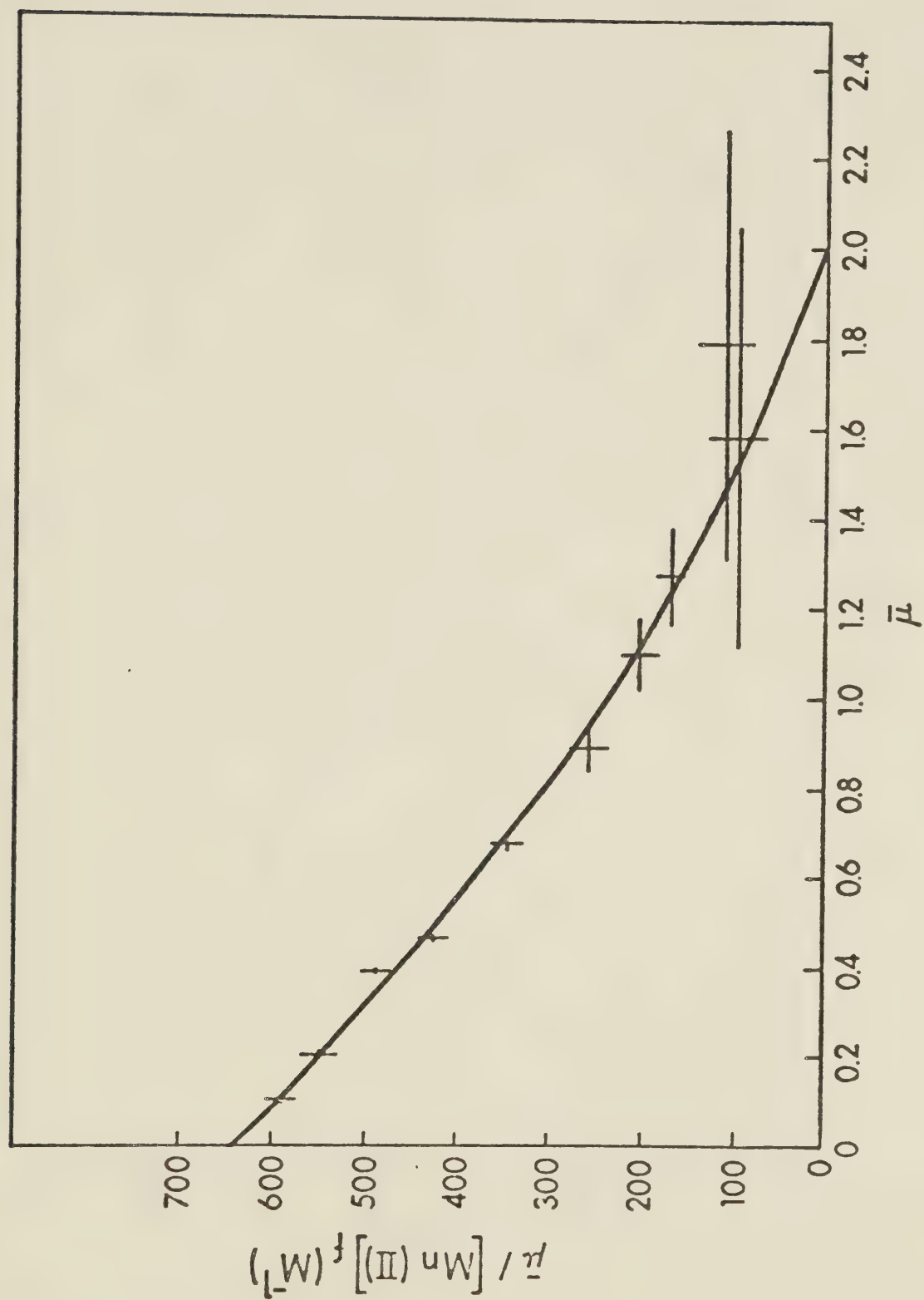


FIGURE 6. The Scatchard plot of the EPR data, corrected for MnCl^+ . Error limits are calculated as for Figure 5.

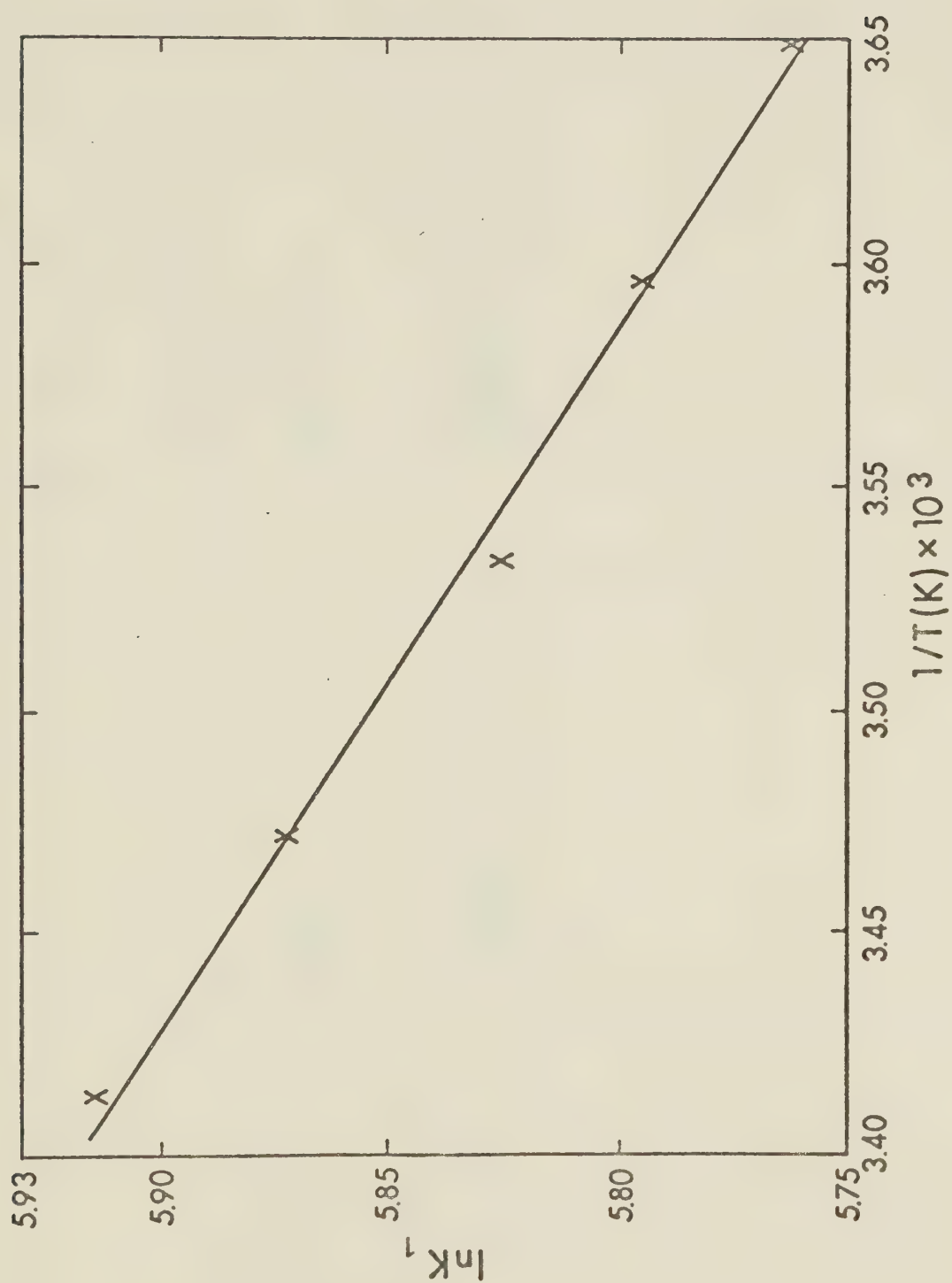


FIGURE 7. Temperature dependence of K_1 for Mn(II)-NADP.

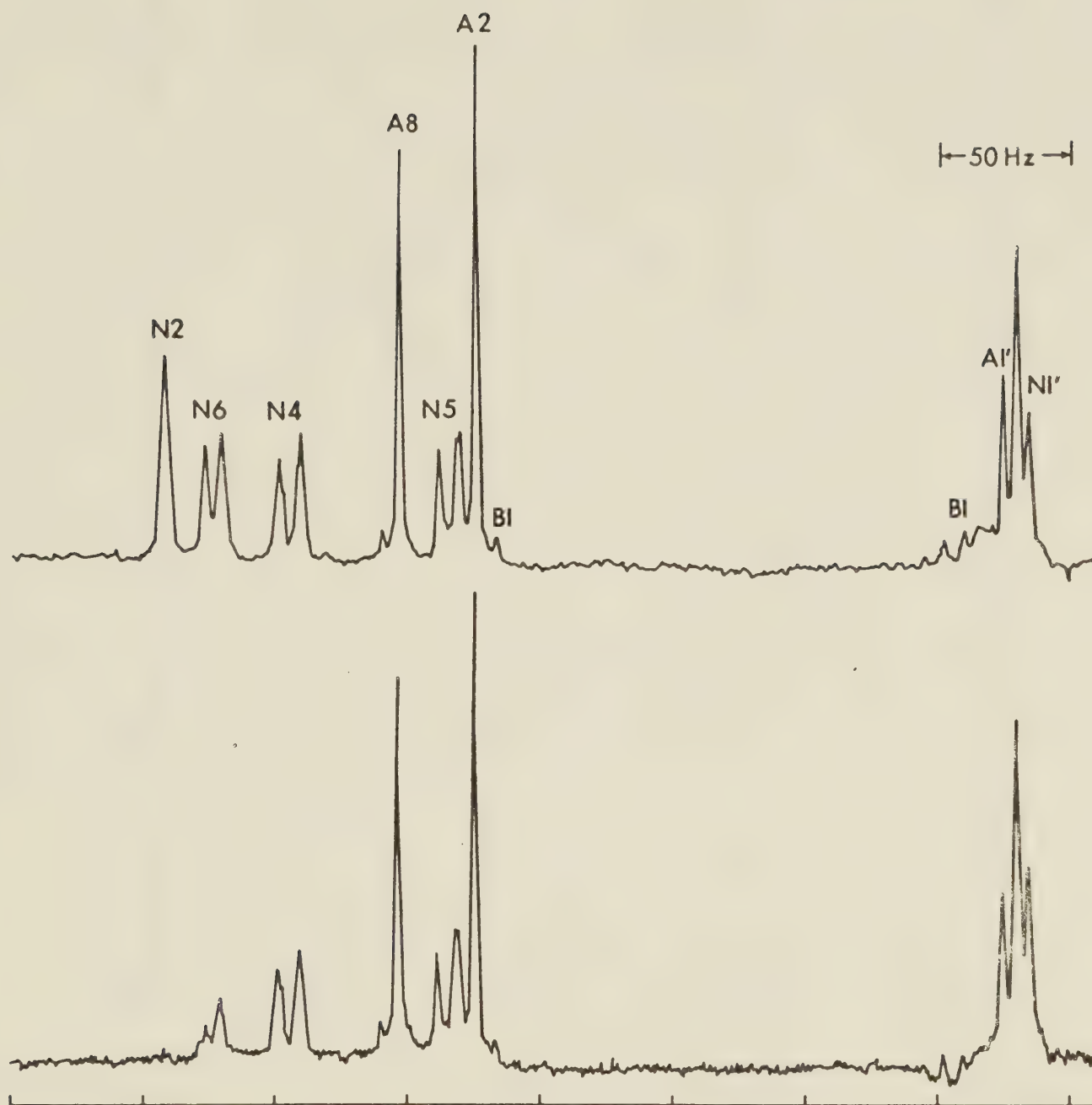


FIGURE 8. The nOe experiment on NADP. The top spectrum is an ordinary spectrum of NADP. All conditions for the bottom spectrum are identical, except that the sample was irradiated at the frequency of the N2 proton resonance. Peaks labelled BI are images of the N-ethyl morpholine resonances at $\delta = 3.1$ and $\delta = 1.4$.

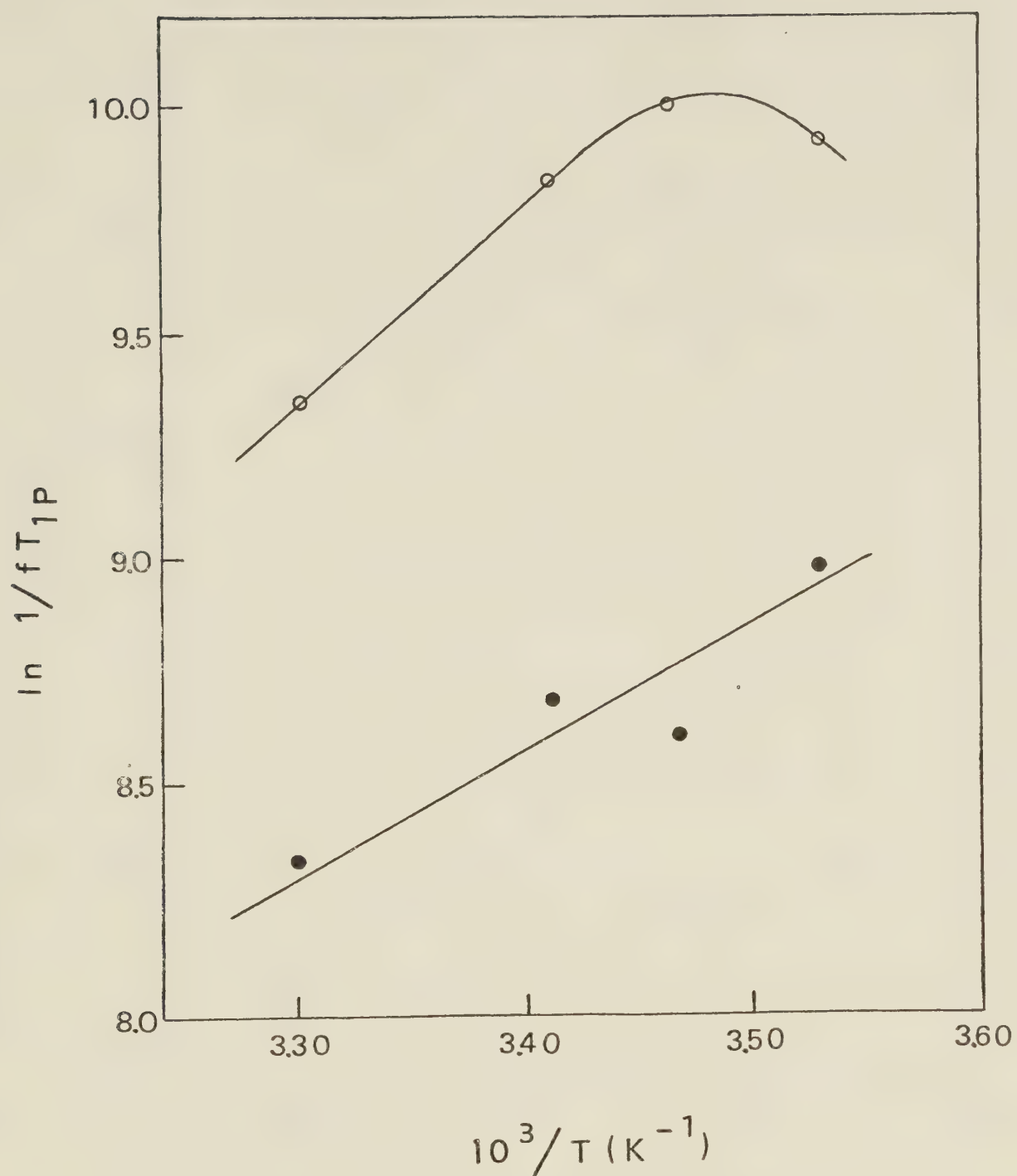


FIGURE 9. A plot of $\ln 1/fT_{1P}$ vs. $1/T$ for the Al' (○) and N1' (●) proton resonances of NADP.

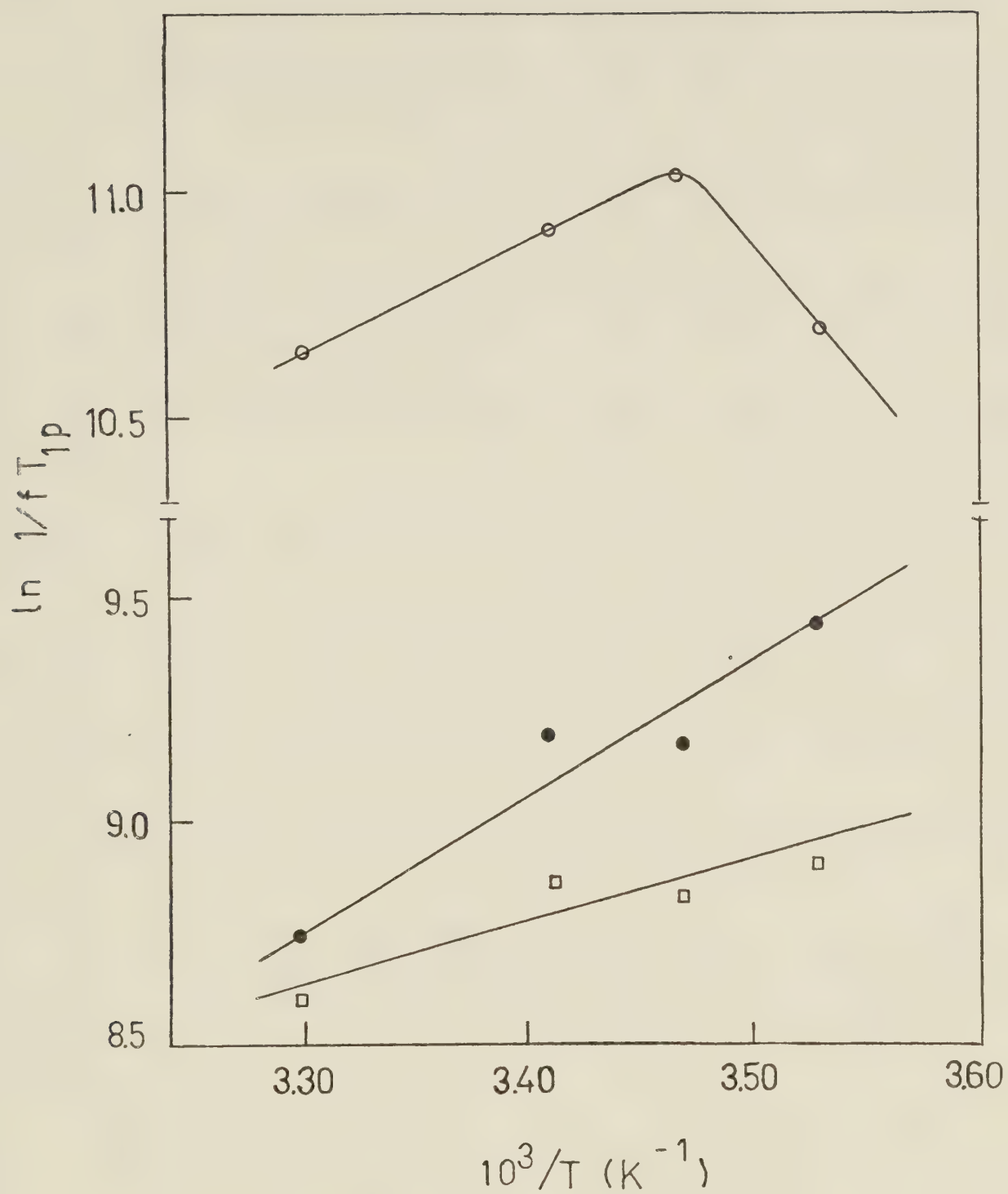


FIGURE 10. A plot of $\ln 1/fT_{1p}$ vs. $1/T$ for the A8(o), A2(●), and N2(□) proton resonances of NADP.

TABLE II. Experimental proton $T_{1,0}$ and $T_{1,Mn}$ data for Mn(II)-NADP solutions together with calculated T_{1M} values (sec) (a)

Sample No.	[Mn(II)] _M		N2	N6	N4	A8	N5	A2	A1'	N1'
1	0	T _{1,0}	.72	.63	1.18	.65	.79	4.22	.98	.53
2	0	T _{1,0}	.70	.43	1.09	.66	.53	3.16	1.02	.65
2	0	T _{1,0}	.66	.50	1.13	.57	.71	3.16	.82	.65
Average		T _{1,0}	.69	.52	1.13	.63	.68	3.51	.94	.47
3	0.5	T _{1,Mn}	.55	.42	1.02	.212	.48	1.12	.41	.48
		T _{1M}	1.87	1.51	7.24	.221	1.13	1.13	.50	2.61
3	0.5	T _{1,Mn}	.49	.40	.76	.176	.54	.96	.41	.46
		T _{1M}	1.17	1.19	1.60	.169	1.31	.91	.50	1.94
4	1.0	T _{1,Mn}	.46	.38	.82	.125	.52	.69	.28	
		T _{1M}	1.93	1.97	4.18	.218	3.09	1.20	.56	
4	1.0	T _{1,Mn}	.40	.37	.70	.134	.43	.50	.27	.39
		T _{1M}	1.33	1.79	2.58	.238	1.63	.82	.53	1.88
5	1.0	T _{1,Mn}	.37	.29	.85	.113	.45	.67	.26	.30
		T _{1M}	1.10	.92	4.73	.190	1.83	1.14	.49	1.14

TABLE II (continued)

6	1.5	$T_{1,Mn}$.36	.30	.67	.092	.51	.47	.25	.39
		T_{1M}	1.56	1.56	3.41	.223	4.23	1.13	.71	2.78
6	1.5	$T_{1,Mn}$.38	.35	-	.099	.38	.51	.23	.34
		T_{1M}	1.86	2.42	-	.243	1.79	1.24	.63	1.84
7	1.5	$T_{1,Mn}$.32	.32	.73	.094	.42	.56	.25	.41
		T_{1M}	1.24	1.73	4.28	.230	2.23	1.38	.71	3.34
8	6.0	$T_{1,Mn}$.185	.192	3.99	.034	-	.137	.089	.215
		T_{1M}	2.09	2.51	5.10	.297	-	1.18	.82	2.92
8	6.0	$T_{1,Mn}$.173	.163	-	-	.105	.149	.077	.275
		T_{1M}	1.90	1.96	-	-	1.02	1.29	.69	5.48
Average $T_{1M}()^{(b)}$			1.61	1.75	4.14	.225	2.03	1.14	.61	2.66
			(.37)	(.50)	(1.70)	(.036)	(1.04)	(.17)	(.11)	(1.25)
%			23	29	41	16	51	15	19	47

(a) The T_{1M} values are multiplied by 10^4 . The temperature is 20°C .

(b) The standard deviation in T_{1M} is designated by .

TABLE III. Experimental ^{31}P $T_{1,0}$ and $T_{1,\text{Mn}}$ data for Mn(II) -NADP solutions together with calculated $T_{1\text{M}}$ values (sec) (a)

Sample No. ^(b)	[Mn(II)] M		PR ^(c)	PL ^(c)	PH ^(c)
1	0	$T_{1,0}$	2.57	1.53	1.39
2	0	$T_{1,0}$	3.16	1.86	1.74
3	0.2	$T_{1,\text{Mn}}$	1.37	1.14	1.20
		$T_{1\text{M}}^{(d)}$	5.2	7.8	7.9
4	0.33	$T_{1,\text{Mn}}$.82	.88	.86
		$T_{1\text{M}}^{(d)}$	8.3	12.2	25.6
5	0.5	$T_{1,\text{Mn}}$.75	.90	.94
		$T_{1\text{M}}^{(d)}$	7.4	15.2	20.8

(a) $T_{1\text{M}}$ values are multiplied by 10^4 .

(b) Samples 1,3, and 5 were run at 146 MHz; samples 2 and 4 were run at 110 MHz.

(c) PR, PL, and PH represent the ^{31}P resonances corresponding to the 2'-ribose phosphate, the low field linkage phosphate, and the high field linkage phosphate, respectively.

(d) $T_{1\text{M}}$ values are calculated using the blank value of $T_{1,0}$ obtained at the same frequency as $T_{1,\text{Mn}}$.

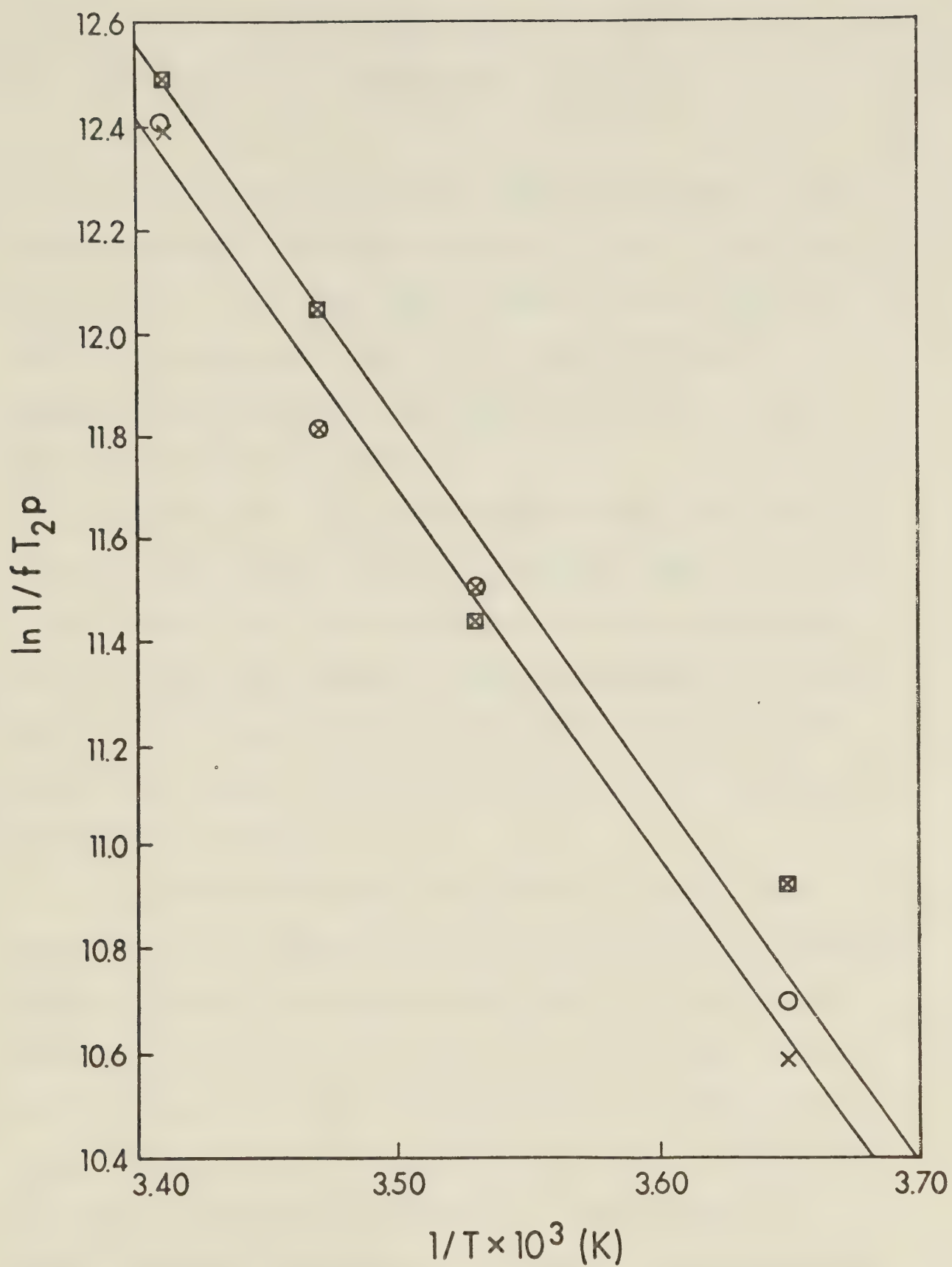


FIGURE 11. Plot of $\ln 1/fT_{2p}$ vs $1/T$ for the ^{31}P nuclei of Mn(II) -NADP. The symbols are: \boxtimes = 2'-phosphate ^{31}P ; \circ = low field linkage ^{31}P ; \times = high field linkage ^{31}P .

CHAPTER FIVE

DISCUSSION

The fit of the uncorrected EPR points (Figure 5) gives apparent macroscopic binding constants of $K_1 = 373 \pm 12 \text{ M}^{-1}$ and $K_2 = 54 \pm 17 \text{ M}^{-1}$. The error limits represent the calculated 99% confidence limits, but a value of $370 \pm 50 \text{ M}^{-1}$ for the first binding constant is probably more appropriate if the experimental error in each point is considered.

This value of K_1 , in the presence of 0.2 M Cl^- ion, is smaller than the values obtained by Maloney and Dennis (1977) and Coleman (1972); 760 M^{-1} and 911 M^{-1} respectively, in the presence of little or no Cl^- ion. However, the value determined in the present study is used in interpreting the NMR results as the NMR and EPR samples were prepared with essentially the same Cl^- ion concentration and ionic strength.

When the EPR points are corrected for the Cl^- ion concentration, as explained in Chapter 3 (Figure 6), the fit appears to improve slightly for points at high values of $\bar{\mu}$, and binding constants of $K_1 = 642 \pm 7 \text{ M}^{-1}$ and $K_2 = 88 \pm 13 \text{ M}^{-1}$ are obtained. As before, the error limits quoted are 99% confidence limits and a more realistic value for K_1 would be $640 \pm 90 \text{ M}^{-1}$. This value of K_1 is in good agreement with the value of 760 M^{-1} reported by Maloney and Dennis (1977) with no Cl^- present, especially considering that the ionic strength employed in the present study is much higher (0.23 as opposed to 0.026). Coleman's corrected value of 1280 M^{-1} (1972) is much higher, and the reason for this unknown.

Maloney and Dennis (1977) and Coleman (1972) did not observe two binding sites for Mn(II) ions on the NADP molecule, but they never considered the possibility, and at low concentrations of Mn(II) ions, it is possible to explain their observations in terms of one binding site.

In order to establish the temperature dependence of K_1 so that the variable f in equations (12) and (13) could be determined for all experiments, a plot of $\ln K_1$ versus $1/T$ was made (Figure 7). This plot shows that the enthalpy of the Mn(II)-NADP interaction is small and positive ($+1.3 \pm 0.1$ Kcal/mol). Values for the two related molecules, adenosine diphosphate (ADP) and adenosine triphosphate (ATP) have been reported to be $+2.6$ Kcal/mole and -4.9 Kcal/mol respectively (Jallon and Cohn, 1970). The value obtained for NADP is much closer to that reported for ADP.

The nOe experiment (Figure 8) ended the uncertainty in the literature concerning the assignment of the anomeric N1' and A1' proton peaks. The assignments for these protons in the literature vary, apparently depending on the experimental conditions (Jardetzky and Wade-Jardetzky, 1966 ; Sarma and Mynott, 1973; Bose and Sarma, 1975).

Egan et al. (1975) observed an nOe in nicotinamide mononucleotide (NMN) of 0.14 for the N1' proton signal when the N2 proton was irradiated and 0.17 when the N6 proton was irradiated at neutral pH and 35°C. In the nOe experiment reported here, the irradiation was centered on the N2 peak position, but this irradiation also saturated most of the N6 signal. Thus an increase in signal intensity of the N1' peak of 30% ($14\% + 17\%$) was observed.

By examining the structure of NADP (Figure 1), the two primary binding sites for Mn(II) ions can be readily located. These are phosphate linkage oxygen atoms and the oxygens of the 2'-phosphate group. The possibility of distinct binding sites at either the nicotinamide C=O oxygen or the adenine N7 nitrogen seems unlikely as these would be much weaker binding sites for the Mn(II) ion than either phosphate group. Although there are obviously two Mn(II) ion binding sites at high Mn(II) ion concentration, it appears that under the conditions of the NMR relaxation measurements, that is when the Mn(II) ion concentration is much less than the NADP concentration, one Mn(II) ion binds simultaneously to both the 2'-phosphate group and the phosphate linkage.

Examination of molecular models shows that it is quite feasible for Mn(II) to bind to both phosphates as long as the adenosine ribose is in the 2'-endo conformation. This idea is further supported by comparison with Mn(II) binding to NAD. If at low concentrations of Mn(II) ions, there are two distinct binding sites, then one of the second microscopic binding constants (the one for Mn(II) ions binding to the species in which one Mn(II) ion is already bound to the 2'-phosphate of NADP) should equal that for Mn(II) ion binding to NAD. However, a separate EPR experiment on the Mn(II)-NAD complex gave the binding constant equal to 26 M^{-1} . This result is inconsistent with the measured second macroscopic binding constant for Mn(II)-NADP of 54 M^{-1} ($1/K_2 = 1/k_1 + 1/k_{12} = 1/k_2 + 1/k_{21}$ and hence k_{12} and k_{21} are both greater than K_2). This implies that only one and not two distinct species of Mn(II)-NADP

TABLE IV. Comparison of T_1 data for NAD and NADP

Proton	Values of Zens et al. (1975, 1976) for 0.005 M NAD at 5°C	Values obtained in present study for 0.005 M NADP		Values obtained in present study, 0.005 M NADP at 30°C	E_a for τ_c (Kcal/mol)
		at 20°C	$T_{1,NADP}$ $T_{1,NAD}$		
N2	0.41	0.70	1.70	0.98	6.0
N6	0.28	0.52	1.86	0.67	4.5
N4	0.66	1.13	1.71	1.46	4.5
A8	0.45	0.63	1.40	0.87	5.7
N5	0.40	0.68	1.70	0.88	4.6
A2	2.13	3.51	1.65	4.57	4.7
N1'	0.32	0.55	1.72	0.74	5.3
A1'	0.87	0.94	1.08	1.18	4.0
					Mean = 4.9 ± 0.4 (a)

(a) The error limits represent one standard deviation.

are present in solution at low Mn(II) ion concentrations.

In addition, the plot of $\ln 1/fT_{2P}$ versus $1/T$ (Figure 11) for the ^{31}P resonance has a straight line with negative slope, indicating that T_{2P} for these nuclei is in the region of slow exchange and therefore $1/fT_{2P}$ equals $1/\tau_M$. All three ^{31}P nuclei have almost the same value of τ_M at 20°C (4×10^{-6} sec) and the same ΔH^\ddagger (13.7 ± 0.5 Kcal/mol). These results are consistent with the one binding site interpretation of the data and argue against two distinct binding sites, namely one at the 2'-phosphate and one at the linkage phosphates. It is unlikely that two binding sites would have the same values of τ_M and ΔH^\ddagger .

It is obvious from equation (9) that a value of τ_R is required in order to carry out distance calculations for the Mn(II)-NADP complex. In order to obtain a reliable value of τ_R , the T_1 values for NADP under the conditions of the present study (0.005 M NADP, pD 8.0, 20°C) were compared with the T_1 data obtained by Ellis and co-workers (Zens et al., 1975, 1976) for NAD under similar conditions (see Table IV). Ellis and co-workers (Zens et al., 1976) measured τ_R for NAD to be 2.8×10^{-10} sec under their conditions (0.005 M NAD, pD 7.0, 5°C). Since $T_1 \propto 1/\tau_c$ for intramolecular dipolar relaxation, the ratio of the T_1 values should allow the calculation of a value for τ_R for NADP, since NADP and NAD are very similar in structure. Table IV indicates that for 6 of the 8 protons which may be compared, $T_{1,\text{NADP}}/T_{1,\text{NAD}}$ is close to 1.7, hence $\tau_{c,\text{NADP}}/\tau_{c,\text{NAD}} = 0.60$ and thus τ_R for NADP is $0.60 \times 2.8 \times 10^{-10}$ sec = 1.7×10^{-10} sec.

The smaller $T_{1,\text{NADP}}/T_{1,\text{NAD}}$ ratios for the A8 and A1'

protons can be attributed to the presence of the 2'-phosphate group in NADP. A1' and A8 are both close to this phosphate and the ^{31}P nucleus may be expected to contribute to their relaxation.

Alternatively, $\tau_{\text{R,NADP}}$ may be calculated from $\tau_{\text{R,NAD}}$ from the mass and temperature dependence of τ_{R} . The Stokes-Einstein equation predicts that for similarly-shaped molecules, $\tau_{\text{R}} \propto$ the molecular mass. Thus, at the same temperature, $\tau_{\text{R,NADP}}/\tau_{\text{R,NAD}}$ equals $\text{mass}_{\text{NADP}}/\text{mass}_{\text{NAD}}$. Furthermore, the temperature dependence of τ_{R} is given by equation (14). The temperature dependence of τ_{R} may be predicted if the rotational correlation activation energy is known.

If $T_1 \propto \tau_{\text{R}}$, and it is known at two temperatures T_a and T_b , then $T_{1,a} = T_{1,b} \exp((E_{\text{R}}/R(1/T_b - 1/T_a)))$ and E_{R} may be determined. Values of T_1 for NADP at 20°C and 30°C have been compared (see Table IV) and yield a mean value of $E_{\text{R}} = 4.9 \pm 0.4$ Kcal/mol. This agrees well with the values of 4.6 ± 0.3 Kcal/mol obtained by Ellis and co-workers (Zens et al., 1975) for NAD. Using an average of 4.75 Kcal/mol for E_{R} gives $\tau_{\text{c}} = 2.8 \times 10^{-10} \times \text{mass}_{\text{NADP}}/\text{mass}_{\text{NAD}} \times \exp(-4750/R(1/278-1/293))$ sec = 2.0×10^{-10} sec for NADP at 20°C. This is reasonably close to the previously calculated value, and the small difference may be caused by the difference in experimental conditions in this work as compared with those of Ellis and co-workers (Zens et al., 1975, 1976). The value of 1.7×10^{-10} sec is used for the subsequent calculations as it is derived from a simple comparison of experimental values.

Although $1/\text{f}T_{1\text{P}}$ for the protons was obtained at only four temperatures, the plots of $1/\text{f}T_{1,\text{P}}$ versus $1/T$ (Figures 9 and 10) indicate that the protons are in the fast exchange region.

Proton A8, which is the proton closest to the slow exchange region, is not in the slow exchange region until the temperature drops below 15°C. Also, a comparison of the magnitudes of fT_{1P} ($= T_{1M} + \tau_M$) for the A8 proton at 20°C (2.25×10^{-5} sec, see Table II) with the value for τ_M of 4×10^{-6} sec obtained from the ^{31}P data shows that τ_M is less than 20% of the value of fT_{1P} under these conditions.

A comparison of the ^{31}P $1/fT_{1P}$ (Table III) and $1/fT_{2P}$ (Figure 11) values shows that for all three nuclei the ratio of $1/fT_{2P}$ to $1/fT_{1P}$ is greater than 13. That is $(T_{1,M} + \tau_M)/M$ is greater than 13 and therefore τ_M is less than 10% of $1/fT_{1P}$. Although the ^{31}P T_{2P} values are in the slow exchange region, the T_{1P} values are in the fast exchange region. Hence the equations for the distance calculations can be applied to the present T_1 data.

The Mn(II) ion to proton distances are given in Table V and those to the phosphorus nuclei are listed in Table VI. These were calculated using equation (10). For the protons, the Mn(II)-adenosine distances are all shorter than the Mn(II)-nicotinamide distances, which is to be expected in light of the location of the binding site. In principle, the Mn(II)-proton distance for A8 should be corrected for the contribution of τ_M to fT_{1P} but this would only shorten the distance calculated by $0.1\overset{\circ}{\text{A}}$, much less than the error quoted in Table IV.

Before a detailed discussion of these distances is made, it is appropriate to consider whether these distances are relevant in considering the solution conformation of free NADP. In order to assess the effect of metal ion binding on the NADP conformation,

TABLE V. T_{1M} values and calculated Mn(II)-proton distances for Mn(II)-NADP

Proton	N2	N6	N4	A8	N5	A2	A1'	N1'
$T_{1M} \times 10^4 (\sigma)$ (a)	1.61 (.37)	1.75 (.50)	4.14 (1.7)	0.225 (.039)	2.03 (1.04)	1.14 (.17)	0.61 (.11)	2.66 (1.25)
$r(\text{\AA}) (\sigma)$ (b)	5.3 (.5)	5.4 (.5)	6.2 (.6)	3.8 (.4)	5.4 (.5)	5.0 (.5)	4.5 (.5)	5.7 (.6)

(a) σ is one standard deviation(b) distances are calculated using $\tau_c = 1.7 \times 10^{-10}$ sec and equation (9).

TABLE VI. T_{1M} values and calculated Mn(II)-phosphorus distances for Mn(II)-NADP.

^{31}P Nucleus ^(a)	PR	PL	PH
$T_{1M} \times 10^4$ (110 MHz)	5.2	7.8	7.8
(146 MHz) ^(b)	7.8	13.8	23.2
$r(\text{\AA})$ (110 MHz)	3.2	3.4	3.4
(146 MHz)	3.4	3.8	4.1
$r_{\text{average}}(\text{\AA})$	3.3	3.6	3.7

(a) PR, PL, and PH represent the ^{31}P resonances corresponding to the 2'-ribose phosphate, the low field linkage phosphate, and the high field linkage phosphate, respectively.

(b) These values are averages of those for samples 3 and 5, Table III.

NMR spectra of 0.003 M NADP in the presence and absence of Mg(II) ions (0.006 M) were obtained. Since the chemistry of Mg(II) and Mn(II) is similar, it is likely that these two ions form similar complexes with NADP. Maloney and Dennis (1977) measured the K_s for the Mg (II)-NADP complex and it is equal to 430 M^{-1} as compared to a K_s for NADP of 760 M^{-1} . Assuming a similar ratio of stability constants under the experimental conditions of the present study, approximately 1/2 of the NADP will be complexed. Differences in the peak positions in the two spectra (with and without Mg(II) ions added) of more than 0.5 Hz were not observed. The chemical shifts of the nicotinamide and adenosine protons are known to shift 0.1-0.3 ppm to high field relative to those of NMN,5'-adenosine monophosphate (5'AMP), and adenosine diphosphoribose (ADPR) due to intramolecular ring current shielding in NADP (Jardetzky and Wade-Jardezky, 1966; Sarma and Mynott, 1973). Any significant change in the spatial relationship of the two rings would be expected to change this ring current shift, and the absence of any difference between the two spectra argues that such a change does not occur on the binding of Mg(II) ions. The possibility of opposing effects (a change in conformer populations to a set of conformers with identical shifts) cannot be ruled out, however. As the ribose region of the spectrum could not be examined in detail at 100 MHz, conclusions cannot be drawn with respect to conformational changes for the rest of the molecule on binding. Nevertheless, it is likely that our conclusions regarding the relative position of the two rings in the complex can be extended to free NADP.

In addition, both rings may be in either the syn or anti

conformation with respect to their contiguous ribose groups. Ellis and co-workers (Zens et al., 1976) found that the adenine ring was 92% anti at 5°C, and that similar molecules had a similar syn to anti ratio in the range 5°C -30°C. For the nicotinamide portion of the molecule, however, the situation is less clear. Ellis and co-workers (Zens et al., 1976) found nearly equal syn and anti populations in NAD, whereas Sarma and Mynott (1973) state that the nicotinamide ring is predominately syn in NAD. On the other hand, Egan et al. (1975) found a slight preference for the anti conformation in NMN. A theoretical study (Thornton and Bayley, 1977) found a slight preference for the syn conformation for the nicotinamide ring in stacked structures of NAD.

In view of these results, the data in Table IV may now be analyzed. The Mn(II)-N4 (6.2 \AA) and Mn(II)-N1' (5.7 \AA) distances are independent of the syn to anti ratio of the nicotinamide ring, and thus these two distances can be used to place the Mn(II) ion approximately 4.5 \AA from the ring centre. The other three nicotinamide distances are all equal ($5.3\text{-}5.4 \text{ \AA}$) and constrain the vector from the ring centre to the Mn(II) ion to within 30° of the normal to the ring plane; that is the Mn(II) ion is located more or less directly above one of the ring faces, but which face it is cannot be determined.

The Mn(II)-A8 (3.8 \AA) and the Mn(II)-A1' (4.5 \AA) distances can be used to place the Mn(II) ion relative to the adenine ring, but the Mn(II)-A2 (5.0 \AA) distance is too short to be consistent with the other two adenosine proton distances. This can be explained in terms of the approximately 90% anti, 10% syn conformation ratio

for the adenine base in similar molecules (Zens et al., 1976). As we are observing a distance that is an average over $1/r^6$, shorter distances are more heavily weighted. Thus, if A2 in the syn conformation is roughly 3.5 \AA away, a value near 5 \AA will be observed even if the A2 proton is much further away in the anti conformation.

The measured Mn(II)-adenosine distances are shorter than those observed for the Mn(II)-ATP system (Mildvan, 1977). The distances for Mn(II)-ATP are: A8, 4.5 \AA ; A1', 6.4 \AA ; and A2, 6.2 \AA . These different distances may be reconciled with those of the present study when we consider the effect of the 2'-ribose phosphate of NADP, which ATP does not have. Space filling models show that if the linkage phosphate-bound Mn(II) ion is to simultaneously bind to the 2'-phosphate group, the adenine must be pulled much closer to the Mn(II) ion in NADP than in ATP.

The calculated Mn(II)- ^{31}P distances (Table V) are 3.3 \AA to the ^{31}P nucleus in the 2'-ribose phosphate group, 3.6 \AA to the linkage phosphorus resonating at lower field, and 3.7 \AA to the linkage phosphorus resonating at higher field. Blumenstein and Raftery (1972) tentatively assign the high field of the AB quartet for the linkage phosphate resonances to the ^{31}P nucleus nearest the adenine base. These ^{31}P to Mn(II) ion distances, together with the Mn(II)-proton distances allow us to consider the conformation of the Mn(II)-NADP complex.

First of all, the Mn(II) ion sits in a pocket between the three phosphates, bound to one oxygen of each of the linkage phosphates and to one or two of the ribose phosphate oxygens. The

adenine ring lies above and is tilted over the plane formed by the three phosphorus atoms, and is close to the Mn(II) ion. The nicotinamide ring is 4.5 \AA away from the Mn(II) ion and faces it. Since the nicotinamide ring can move in an arc with respect to the Mn(II) ion, a family of conformations is possible, ranging from one in which both rings are parallel and $7\text{-}8 \text{ \AA}$ apart to one in which the rings are roughly perpendicular and close to each other. Conformations with close and perpendicular rings may be ruled out as in dinucleotides and other systems such as DNA, the base planes are always parallel to each other. Hence in the Mn(II)-NADP complex there is essentially no close stacking of the rings.

Although it must be remembered that we are measuring time averaged distances for a molecule which is thought to exist in an equilibrium of folded and extended forms when not bound (Jardetzky and Wade-Jardetzky, 1966; McDonald et al., 1972), our measurements are not consistent with the existence of an equilibrium involving an extended and a folded form with closely stacked rings unless the folded form exists only a few percent of the time.

For free NADP, Sarma and Mynott (1973) concluded that in the folded form, the two rings are stacked 3.5 \AA apart, which is not in agreement with the conclusion reached in the present study. On the other hand, Ellis and co-workers (Zens et al., 1976) concluded, based on the absence of any effect of adenine deuteration on the nicotinamide proton T_1 values that the two rings in NAD are at least 4.5 \AA apart and therefore there is no significant stacking of the rings in NAD. This conclusion is consistent with

the results of the present study for NADP. One drawback in the work of Zens et al. (1976) is that if NAD is folded roughly 20% of the time (Jardetzky and Wade-Jardetzky, 1966; McDonald et al., 1972) the time-averaged distance measured by Zen et al. (1976) would be greater than 4.5 Å even if the rings are 3.5 Å apart in the folded form.

In conclusion, the Mn(II) ion in the Mn(II)-NADP complex is bound simultaneously to both phosphate groups, and the two rings are about 7-8 Å apart from each other in the complex. It appears that there is no significant stacking of the rings in the complex, and this conclusion may be extended, with reservations, to the free NADP molecule.

There is much work which could be done to further elucidate the nature of the Mn(II)-NADP complex and to show the relevance of the results obtained in the present study to the conformation of free NADP. Similar work to that already carried out on the aromatic protons should be carried at frequencies above 100 MHz in order to determine distances to the ribose protons, which cannot be resolved at 100 MHz. Alternatively, repeating the $T_{1\rho}$ measurements with a suitable shift reagent added in addition to the Mn(II) ions might prove useful in analysing the ribose region of the spectrum, providing that the effect of these shift reagents on the conformation could be evaluated.

Another high frequency study which might be of interest would be to search for changes in the ribose region of the spectrum on binding of Mg(II) to NADP in order to determine what, if any, conformational changes are induced by metal ion binding.

BIBLIOGRAPHY

- Blumenstein, M. and Raftery, M. A. (1972), Biochemistry 12, 3585-3590.
- Bose, K. S. and Sarma, R. H. (1975), Biochem. Biophys. Res. Comm. 66, 1173-1179.
- Cohn, M. and Townsend, J. (1954), Nature 173, 1090-1091.
- Coleman, R. F. (1972), Anal. Biochem. 46, 358-363.
- Connick, R. E. and Fiat, D. (1966), J. Chem. Phys. 44 4103-4107.
- Czeisler, J. L. and Hollis, D. P. (1975), Biochemistry 14, 2781-2785.
- Deranleau, D. A. (1969), J. Amer. Chem. Soc. 91, 4050-4054.
- Dwek, R. A. (1975), in NMR in Biochemistry, Clarendon Press, Oxford.
- Egan, W., Forsen, S., and Jacobus, J. (1975), Biochemistry 14, 735-742.
- Gryzbowski, A. K., Tate, S. S., and Datta, S. P. (1970), J. Chem. Soc. Sec. A, 241-245.
- Jallon, J. M. and Cohn, M. (1970), Biochem Biophys. Acta. 222, 542-545.
- Jardetzky, O. and Wade-Jardetzky, N. G. (1966), J. Biol. Chem. 241 85-91.
- Lehninger, A. L. (1970), in Biochemistry, Worth, New York, N. Y..
- Lumry, R., Smith, E. L., and Glantz, R. R. (1951), J. Amer. Chem. Soc. 73, 4330-4340.
- Luz, E. and Meiboom, S. (1964), J. Chem. Phys. 40, 2686-2692.
- Maloney, R. J. and Dennis, D. T. (1977), Can. J. Biochem. 55, 928-934.
- McDonald, G., Brown, B., Hollis, D. P., and Walter, C. (1972), Biochemistry 11, 1920-1930.
- Mildvan, A. S. and Gupta, R. K. (1978), Meth. Enz. 49, 332-359.

- O'Sullivan, W. J. and Cohn, M. (1966), J. Biol. Chem. 241, 3104-3415.
- Pabst Laboratories (1956), UV Spectra of 5'-Ribonucleotides, Circular OR-10.
- Reed, G. H., Leigh, J. S., and Pearson, J. E. (1971), J. Chem. Phys. 55, 3311-3316.
- Reuben, J., Reed, G. H., and Cohn, M. (1970), J. Chem. Phys. 52, 1617.
- Rubenstein, M., Baram, A., and Luz, Z. (1971), Mol. Phys. 20, 67-80.
- Saenger, W., Reddy, B. S., Muegger, K., and Weimann, G. (1977), Nature 267, 225-229.
- Sarma, R. H. and Mynott, R. J. (1972), Org. Mag. Res. 4, 577-584.
- Sarma, R. H. and Mynott, R. J. (1973), in Conformation of Biological Molecules and Polymers, The Jerusalem Symposia on Quantum Chemistry and Biochemistry, (Bergmann, E. D. and Pullman, B., Eds.), Vol. 5, The Israel Academy of Sciences and Humanities, Jerusalem.
- Sloan, D. L. and Mildvan, A. S. (1976), J. Biol. Chem. 251, 2412-2420.
- Solomon, I. (1955), Phys. Rev. 99, 559-565.
- Solomon, I. and Bloembergen, N. (1956), J. Chem. Phys. 25, 261-266.
- Swift, T. J. (1973), in NMR of Paramagnetic Molecules, (LaMar, G. N., Horrocks, W. DeW., and Holm, R. H., Eds.), Academic Press, New York, N. Y..
- Swift, T. J. and Connick, R. E. (1962), J. Chem. Phys. 37, 307-320.
- Thornton, J. M. and Bayley, P. M. (1977), Biopolymers 16, 1971-1986.
- Torreilles, J. and Crastes de Paulet, A. (1973), Biochimie 55, 1077-1083.

Torreilles, J., Crastes de Paulet, A., and Platzner, N. (1977), Org. Mag. Res. 9, 584-588.

Villafranca, J. J. and Mildvan, A. S. (1971), J. Biol. Chem. 246, 5791-5797.

Zens, A. P., Bryson, T. A., Dunlap, R. B., Fisher, R. R., and Ellis, P. D. (1976), J. Amer. Chem. Soc. 98, 7559-7564.

Zens, A. P., Williams, T. J., Wisowaty, J. C., Fisher, R. R., Bryson, T. A., and Ellis, P. D. (1975), J. Amer. Chem. Soc. 97, 2850-2857.

B30234